Journal of chemical & engineering data

pubs.acs.org/jced Article

Investigation of Mixed MEA-Based Solvents Featuring Ionic Liquids and NMP for CO_2 Capture: Experimental Measurement of CO_2 Solubility and Thermophysical Properties

Mojgan Ebrahiminejadhasanabadi, Wayne Michael Nelson,* Paramespri Naidoo, Amir H. Mohammadi, and Deresh Ramjugernath

Cite This: *J. Chem. Eng. Data* 2021, 66, 899–914 Read Online

ACCESS | Metrics & More | Article Recommendations

ABSTRACT: Alkanolamine solutions are used in the industry worldwide to remove carbon dioxide and hydrogen sulfide from natural gas, but such technologies have disadvantages. This study aimed to investigate the new hybrid amine solvents for carbon dioxide capture and their potential to reduce the disadvantages of amine technology. The solubility of carbon dioxide in hybrid solvents with different mixtures of monoethanolamine, water, *n*-methyl-2-pyrrolidone, 1-butyl-3-methylimidazolium trifluoromethanesulfonate, and 1-butyl-3-methylimidazolium bis(trifluoromethanesulfonyl)imide was measured at temperatures of 298.15 and 313.15 K by a static synthetic method. The viscosity, density, speed of sound, and evaporation rates for the hybrid solvents were also measured. Experimental observations indicate that the solubility of carbon dioxide in a hybrid solvent of *n*-methyl-2-pyrrolidone + monoethanolamine was greater than that of the aqueous amine solvent, except at low pressures depending on the concentration of amine. The addition of an ionic liquid to the amine solution reduced the volatility of the solvent and decelerated the evaporation rate of amine, while the loss of ionic liquid was almost zero. However, the addition of an ionic liquid to *n*-methyl-2-pyrrolidone-containing monoethanolamine solvent or the aqueous monoethanolamine solvent decreased the solubility of carbon dioxide and increased the viscosity of the solution.

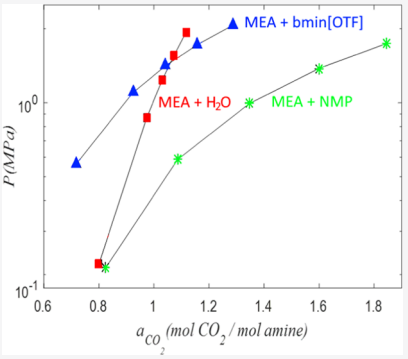

1. INTRODUCTION

Natural gas is the Earth's cleanest-burning hydrocarbon and the most environmentally friendly fossil fuel compared to oil and coal.[1,2] The International Energy Agency (IEA) predicts a 30% increase in energy demand from 2017 to 2040,[3] which means the demand for natural gas will increase. In 2016, the annual growth of natural gas demand was 1.9%.[4] Natural gas contains several impurities, in particular carbon dioxide (CO_2) and hydrogen sulfide (H_2S) that form corrosive acidic solutions in the presence of water.[1,5−8] The use of absorption processes with alkanolamine solutions in removing H_2S and CO_2 is common in the industry, with drawbacks in this technology being amine solvent loss, corrosion, and high heat consumption.[1,9−13] The replacement of existing amine units worldwide with new technologies may not be economically practical. However, altering the composition of the amine solvents would not require considerable process and equipment modifications.[14] For example, the use of hybrid solvents, containing amine solutions and physical solvents, may improve the efficiency of the current amine absorption processes. Hybrid solvents couple the properties of solvents to take advantage of favorable aspects of solvents while minimizing the disadvantages.[15,16] In recent years, ionic liquids (ILs), which are nonvolatile and recyclable solvents,[1,9,17−19] have been investigated as blends with amines and other physical solvents for carbon dioxide capture.[12−14,16,20−45] Lei et al.[43] showed that addition of omim[TF_2N] to methanol at a temperature of 313.2 K and pressures between 2 and 6 MPa increases the CO_2 solubility in comparison to pure methanol.[43] Bernard et al.[21] indicated that the addition of bmim[BF_4] to the aqueous monoethanolamine (MEA) solution reduces the corrosion of process equipment, which is one of the main disadvantages of the amine process.[21] Furthermore, addition of an IL may help reduce the energy consumption for regeneration of amine solutions,[20,22−24,29] while also increasing the absorption rate.[12,13,25−28] Haghtalab and Shojaeian[20] showed that the enthalpy of solution of CO_2 in the MDEA + bmim[acetate] solution is about half of the enthalpy of solution of CO_2 in the aqueous MDEA. It was concluded that replacing the aqueous media of the amine solution by the IL reduces the energy

Received: July 6, 2020
Accepted: December 7, 2020
Published: January 15, 2021

Table 1. Pure-Component Parameters, Purities, and Properties of the Chemicals Used in This Study, as well as the Expanded Uncertainty (k = 2)

		density (g/cm^3)		refractive index			
component	supplier	experimental[a]	literature[b]	experimental[c]	literature[d]	supplier purity (wt %)	purification
CO_2	Afrox	NA	NA	NA	NA	99	none
NMP	Merck	1.0119 (at 318.15 K)	1.0117 (at 318.15 K)	1.469 (at 298.15 K)	1.4680 (at 298.15 K)	≥99.5	dried
MEA	Sigma-Aldrich	1.0105 (at 303.15 K)	1.009 (at 303.15 K)	1.4513 (at 298.15 K); 1.4532 (at 293.15 K)	1.4521 (at 298.15 K); 1.4539 (at 293.15 K)	≥99	dried
H_2O	obtained from a Q5 Ultrapure (Millipore) purifier	0.9957 (at 303.15 K)	0.9957 (at 303.15 K)	1.3325 (at 298.15 K); 1.333 (at 293.15 K)	1.3325 (at 298.15 K) 1.3330 (at 293.15 K)		degassed
bmim[OTF]	Sigma-Aldrich	1.2833 (at 313.15 K)	1.2945 (at 313.15 K)	1.4383 (at 298.15 K); 1.4395 (at 293.15 K)		97	dried
bmim[TF_2N]	Sigma-Aldrich	1.4162 (at 318.15 K); 1.4353 (at 298.15 K)	1.440 (at 298.15 K)	1.4266 (at 298.15 K); 1.4281 (at 293.15 K)		≥98	dried

[a]$U(T)$ = 0.02 K; $U_r(\rho)$ = 0.004, data recorded at 0.101 MPa, $U(P)$ = 0.001 MPa. [b]Data for the liquid density (ρ) from the literature.[45,70,75−77] [c]$U(T)$ = 0.02 K; $U(n_D)$ = 0.001; data recorded at 0.101 MPa and a standard wavelength of 589 nm, $U(P)$ = 0.001 MPa. [d]Data for the refractive index (n_D) from the literature.[66,78]

required for the solvent regeneration.[20] Baj et al. studied the CO_2 solubility in the hybrid solvents of the MEA, water, and eight ILs including 1-butyl-3-methylimidazolium trifluoromethanesulfonate (bmim[OTF]) with an initial loading concentration of $w_{bmim[OTF]}/w_{MEA}$ = 0.3500/0.3000, at atmospheric pressure and a temperature of 298.15 K.[12] It was concluded that solvents involving water/IL/MEA had the potential to capture CO_2.[12] The presence of water in aqueous solvents poses some disadvantages for amine processes as it has a high heat capacity, which increases the energy consumption of the amine technology, and CO_2 and H_2S form acidic solutions in the presence of water.[6] A further concern is the volatility of amine solutions, which could lead to the release of amine and water into the gas phase and air during the desorption process, resulting in solvent loss and replenishment costs.[9,46] Thus, the use of alternate physical solvents as a substitute for the aqueous media of amine solutions to reduce the problems of the amines was investigated in this study. With this aim, the ILs, namely, bmim[OTF] and 1-butyl-3-methylimidazolium bis-(trifluoromethanesulfonyl)imide (bmim[TF_2N]), and n-methyl-2-pyrrolidone (NMP) were chosen based on the comparison study performed on their ability to absorb the acidic gases, availability, volatility, viscosity, and selectivity toward H_2S.[1,19,47−49] Additionally, the primary amine MEA was selected as it exhibits a higher heat reaction, degradation products, corrosive problems, and solvent loss.[50−55] New solubility data were measured for CO_2 in MEA + H_2O + bmim[OTF] and MEA + NMP + bmim[TF_2N] mixtures at temperatures of 298.15 and 313.15 K. Viscosity, speed of sound, and density for the liquid solvents were measured over the temperature range of 293.15−333.15 K. The evaporation rates of the solvents were measured at 373.15 K. The evaporation rates were measured to provide a comparison of the volatility of the solvents.

2. EXPERIMENTAL SECTION

2.1. Materials. Carbon dioxide (CAS number: 124-38-9) was purchased from Afrox (South Africa) with a minimum mass fraction purity of 0.99. MEA (CAS number: 141-43-5), bmim[OTF] (CAS number: 174899-66-2), and bmim[TF_2N] (CAS number: 174899-83-3) were purchased from Sigma-Aldrich with stated mass fraction purities ≥0.99, 0.97, and ≥0.98, respectively. NMP (CAS number: 872-50-4) was purchased from Merck with stated mass fraction purity ≥0.995. The pure-component physical properties are listed

Table 2. Standard Uncertainty Estimates and Influences of the Variables in This Work

source of uncertainty	distribution	estimate
Pressure (P)		
P reference (MPa): Mensor CPC 8000 (25 MPa)	normal	0.0025
correlation for P (MPa), (4 MPa), equilibrium cell	rectangular	0.0003
correlation for P (MPa), (2.5 MPa), gas reservoir	rectangular	0.0001
Temperature (T)		
T reference (K): CTH 6500	rectangular	0.02
correlation for T (K), equilibrium cell (EC)	rectangular	0.02
correlation for T (K), gas reservoir (GR)	rectangular	0.01
Volume of Gas Phase (V_g) in Equilibrium Cell		
total volume of equilibrium cell (cm^3)	none[a]	$u(V_{EC})$ = 0.03
calibration of the depth gauge, V^L (cm^3)	rectangular	0.09
repeatability of volume (cm^3)	rectangular	0.12
liquid density (g/cm^3)	rectangular	0.0002
Total Composition[b] (z_i)		
pressure (MPa), gas reservoir	none[a]	$u(P_{GR})$ = 0.0008
temperature (K), gas reservoir	none[a]	$u(T_{GR})$ = 0.01
total volume of gas reservoir (cm^3)	none[a]	$u(V_{GR})$ = 0.05
compressibility factor vapor phase, Z^V	rectangular	$0.006Z^V$
mass balance uncertainty[c] (g)	rectangular	0.03
mass balance uncertainty[d] (g)	rectangular	0.003
CO_2 Solubility and Liquid Phase Composition[e] (x_i)		
pressure (MPa), equilibrium cell	none[a]	$u(P_{EC})$ = 0.0009
temperature (K), equilibrium cell	none[a]	$u(T_{EC})$ = 0.02
vapor phase composition	rectangular	$1 - y_{CO_2}$
volume of gas phase, V_g (cm^3)	none[a]	$u(V_g)$ = 0.09
compressibility mixture vapor phase (Z^V)	rectangular	$0.006Z^V$

[a]Combined standard uncertainty. [b]Total composition of the mixture prepared in the equilibrium cell. [c]Mass balance uncertainty for loading a known mass of liquid into the equilibrium cell. [d]Mass balance uncertainty for preparing solvent mixtures. [e]Composition of the liquid phase calculated from the $T-P-z$ data.

https://dx.doi.org/10.1021/acs.jced.0c00618
J. Chem. Eng. Data 2021, 66, 899−914

Table 3. Overview of the Liquid Mixtures and Respective Measurements Presented in This Work

initial mass composition	temperature (K)	pressure range (MPa)
CO_2 Solubility Measurement		
MEA (1) + H_2O (2) + bmim[OTF] (3):	298.15 and 313.15	0.093−2.322
w_1/w_2 = 0.2965/0.7035 $w_1/w_2/w_3$ = 0.2980/0.6017/0.1003 $w_1/w_2/w_3$ = 0.2994/0.4614/0.2392 $w_1/w_2/w_3$ = 0.2924/0.3071/0.4005		
MEA + (NMP + bmim[TF_2N])/H_2O/bmim[OTF]:	313.15	
1- MEA (1) + H_2O (2): w_1/w_2 = 0.1034/0.8966 w_1/w_2 = 0.1997/0.8003 w_1/w_2 = 0. 2965/0.7034		0.189−2.322
2- MEA (1) + NMP (2): w_1/w_2 = 0.1025/0.8975 w_1/w_2 = 0.2032/0.7968 w_1/w_2 = 0.3037/0.6963		0.194−2.298
3- MEA (1) + bmim[OTF] (2): w_1/w_2 = 0.0912/0.9088		0.564−2.065
4- MEA (1) + NMP (2) + bmim[TF_2N] (3): $w_1/w_2/w_3$ = 0.1039/0.7966/0.0995 $w_1/w_2/w_3$ = 0.0977/0.6492/0.2531 $w_1/w_2/w_3$ = 0.1162/0.4932/0.3906		0.297−1.993
Viscosity, Density, and Sound Velocity Measurement		
MEA (1) + H_2O (2) + bmim[OTF] (3):	293.15−333.15	0.101
w_1/w_2 = 0.3004/0.6996 $w_1/w_2/w_3$ = 0.3119/0.5836/0.1045 $w_1/w_2/w_3$ = 0.2994/0.4614/0.2392 $w_1/w_2/w_3$ = 0.3046/0.2643/0.4311		
MEA + (NMP + bmim[TF_2N])/H_2O/bmim[OTF]:	293.15−333.15	0.101
1- MEA (1) + H_2O (2): w_1/w_2 = 0.1034/0.8966 w_1/w_2 = 0.2008/0.7992 w_1/w_2 = 0.3004/0.6996		
2- MEA (1) + NMP (2): w_1/w_2 = 0.1021/0.8979[a] & 0.1025/0.8975[b] w_1/w_2 = 0.2090/0.7910[a] & 0.1990/0.8010[b] w_1/w_2 = 0.3089/0.6911[a] & 0.3074/0.6926[b]		
3- MEA (1) + bmim[OTF] (2): w_1/w_2 = 0.0912/0.9088		
4- MEA (1) + NMP (2) + bmim[TF_2N] (3): $w_1/w_2/w_3$ = 0.0976/0.8032/0.0992 $w_1/w_2/w_3$ = 0.1138/0.6414/0.2448 $w_1/w_2/w_3$ = 0.1162/0.4932/0.3906		
Evaporation Rate Measurement		
MEA (1) + H_2O (2) + bmim[OTF] (3): w_2/w_1 = 0.6996/0.3004 $w_3/w_2/w_1$ = 0.1045/0.58336/0.3119 $w_3/w_2/w_1$ = 0.2492/0.458/0.2928 $w_3/w_2/w_1$ = 0.3943/0.3178/0.2879	373.15	0.101
MEA + (NMP + bmim[TF_2N])/H_2O/bmim[OTF]:	373.15	0.101
1- MEA (1) + H_2O (2): w_1/w_2 = 0.0997/0.9003 w_1/w_2 = 0.1985/0.8015 w_1/w_2 = 0.3004/0.6996		
2- MEA (1) + NMP (2): w_1/w_2 = 0.1129/0.8871 w_1/w_2 = 0.2070/0.793 w_1/w_2 = 0.3050/0.695		
3- MEA (1) + bmim[OTF] (2): w_1/w_2 = 0.0912/0.9088		
4- MEA (1) + NMP (2) + bmim[TF_2N] (3): $w_1/w_2/w_3$ = 0.1039/0.7966/0.0995 $w_1/w_2/w_3$ = 0.0977/0.6492/0.2531 $w_1/w_2/w_3$ = 0.1162/0.4932/0.3906		

[a]Viscosity measurements. [b]Density and sound velocity measurements.

in Table 1. The ILs were evacuated at 363.15 K for 3 days. MEA and NMP were dried under vacuum at 323.15 K for 6 h to remove trace quantities of water and volatiles. The refractive index of the liquid components was measured using a commercial digital refractometer (Atago, RX-7000α).

2.2. Viscosity, Density, Speed of Sound, and Evaporation Rate Measurements. The viscosity, density, and speed of sound for the liquid solvents and blends were measured using a commercially available analytical apparatus (Anton Paar, DSA 5000M) equipped with an auxiliary viscometer (Lovis, 2000ME). Calibration of the device was out-sourced. The viscosity, density, and speed of sound measurements were performed simultaneously at isothermal conditions and pressure of 0.101 MPa using a single sample (volume, 3.5 cm^3). Uncertainties for temperature, density, viscosity, and speed of sound were $U(T)$ = 0.02 K, $U_r(\rho)$ = 0.004, $U_r(\eta)$ = 0.004, and $U(c)$ = 0.7 $m{\cdot}s^{-1}$, respectively. A thermogravimetric analyzer (TGA) (Shimadzu; DTG-60AH) was used to measure the evaporation rates of the solvents. The experiments were performed at a pressure of 0.101 MPa. A constant flow of 100 cm^3/min of nitrogen (Afrox, N5.0) was maintained throughout the experiment. The instrument simultaneously measures the difference in mass and temperature between the sample and an inert standard substance. In this case, the furnace was heated to 373.15 K and held constant, while the mass of the sample was recorded as a function of time. When the rate of change in the mass of the sample remained zero for at least 1 h, the measurement was stopped. The change in mass of the sample with respect to time was then used to obtain the evaporation rate of the sample.

2.3. Carbon Dioxide Solubility Measurements. A static synthetic apparatus was used to measure the solubility of CO_2 in the hybrid solvents. The experimental apparatus was described in detail in a previous study.[56] The core of the apparatus features a transparent equilibrium cell constructed from a sapphire tube. The volume of the cell was previously determined to be 36.29 cm^3. The equilibrium cell contains an internal mixer. The cell was maintained at a constant temperature by submerging into a temperature-controlled liquid bath. The temperature and pressure within the cell were measured using two 100-ohm platinum resistance (Pt-100) probes (WIKA; 1/10 DIN) and a single pressure transmitter (WIKA; P-30; 4 MPa), respectively. The liquid level within the equilibrium cell was determined visually using a depth gauge and digital caliper. The apparatus also features an isothermal gas reservoir with a capacity of 137.09 cm^3.

The solvent mixtures were prepared gravimetrically using a digital mass balance (Ohaus Explorer; maximum capacity, 450 g; readability, 0.001 g). The mixture preparation and handling were performed under vacuum, within glass round-bottom flasks, to minimize exposure to the atmosphere. The solvent was loaded into the evacuated equilibrium cell, and the mass of solvent was determined gravimetrically (Ohaus Pioneer Precision; maximum capacity, 4200 g; readability, 0.01 g). CO_2 was then metered from the isothermal gas reservoir into the equilibrium cell. The temperature and pressure within the gas reservoir were measured by a single Pt-100 probe and a

https://dx.doi.org/10.1021/acs.jced.0c00618
J. Chem. Eng. Data 2021, 66, 899−914

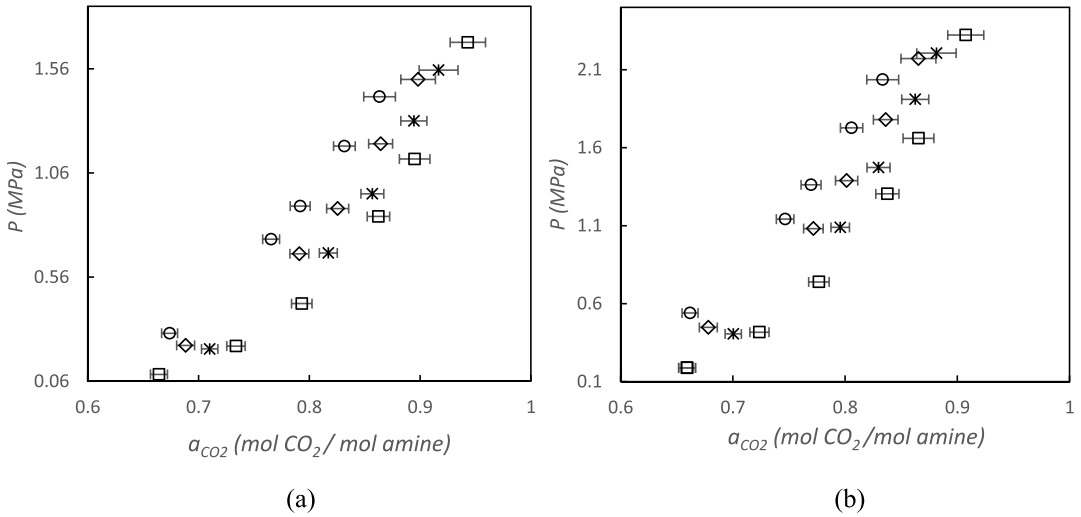

Figure 1. Solubility data of CO_2 in MEA (1) + H_2O (2) + bmim[OTF] (3) with different mass compositions: w_2/w_1 = 0.7035/0.2965 (□), $w_3/w_2/w_1$ = 0.1003/0.6017/0.2980 (*), $w_3/w_2/w_1$ = 0.2392/0.4614/0.2994 (◇), and $w_3/w_2/w_1$ = 0.4005/0.3071/0.2924 (○) at (a) 298.15 K and (b) 313.15.

Table 4. Experimental (exp) Data of the Solubility of CO_2 in Solvent of MEA (1) + H_2O (2) with w_1 = 0.2965, Including the Measured Temperature (T), Pressure (P), Volume of Gas Phase (V_g), Total Number of Moles of Solvent ($n_{solvent}$), Number of Moles of CO_2 (n_{CO_2}), Total Mole Fraction of CO_2 (z_{CO_2}), Apparent Mole Fraction of CO_2 in Liquid Phase[a] (x_{CO_2}), and Solubility of CO_2[b] (a_{CO_2}), Including the Expanded Uncertainties (k = 2), $U(T)$ = 0.02 K, $U(P)$ = 0.002 MPa, and $U(w)$ = 0.0001

T (K)	P(MPa)	V_g(cm^3)	n_{CO_2} (mol)	$n_{solvent}$ (mol)	z_{CO_2}	$U(z_{CO_2})$	$x^{exp}_{CO_2}$	$U(x_{CO_2})$	$a^{exp}_{CO_2}$	$U(a_{CO_2})$
313.10	0.189	15.00	0.0676	0.9128	0.0690	0.0007	0.0680	0.0007	0.6592	0.0074
313.09	0.188	15.00	0.0676	0.9128	0.0690	0.0007	0.0680	0.0007	0.6593	0.0076
312.99	0.417	14.93	0.0755	0.9128	0.0764	0.0008	0.0741	0.0008	0.7237	0.0085
313.00	0.739	14.84	0.0828	0.9128	0.0831	0.0008	0.0791	0.0009	0.7767	0.0091
312.98	1.304	14.72	0.0924	0.9128	0.0919	0.0009	0.0848	0.0009	0.8377	0.0103
313.01	1.660	14.68	0.0975	0.9128	0.0965	0.0012	0.0874	0.0013	0.8654	0.0137
312.98	2.322	14.57	0.1063	0.9128	0.1043	0.0014	0.0912	0.0015	0.9075	0.0161
298.05	0.093	15.17	0.0676	0.9128	0.0690	0.0007	0.0684	0.0007	0.6643	0.0077
298.06	0.229	15.06	0.0755	0.9128	0.0764	0.0008	0.0751	0.0008	0.7338	0.0083
298.04	0.433	14.99	0.0828	0.9128	0.0831	0.0009	0.0807	0.0009	0.7932	0.0092
298.05	0.851	14.85	0.0924	0.9128	0.0919	0.0009	0.0871	0.0009	0.8624	0.0101
298.04	1.127	14.77	0.0975	0.9128	0.0965	0.0012	0.0901	0.0013	0.8951	0.0138
298.05	1.687	14.69	0.1063	0.9128	0.1043	0.0014	0.0945	0.0015	0.9431	0.0160

[a] $x_{CO_2} = \frac{n^L_{CO_2}}{n^L_{CO_2} + n_{solvent}}$. [b] $a_{CO_2} = \frac{n^L_{CO_2}}{n^t_{amine}}$.

pressure transmitter (WIKA; P-30; 2.5 MPa), respectively. The number of moles of CO_2 charged into the equilibrium cell was determined using the Peng−Robinson (PR) equation of state (EoS) using the pressure and temperature of the gas reservoir before and after loading. At this point, the total composition of the mixture within the equilibrium is known. The mixture was agitated at a constant temperature, and equilibrium was generally obtained within 12 h of rapid mixing. At equilibrium, the height of the liquid level was measured with the depth gauge and the volumes of the coexisting phases at equilibrium were determined. Finally, the solubility of CO_2 (a_{CO_2}) in the solvent was calculated as

$$a_{CO_2} = \frac{n_{CO_2} - y_{CO_2} V_g \rho_{g,EOS}}{n^t_{amine}} \quad (1)$$

where V_g and $\rho_{g,EOS}$ are the volume and molar density of gas phase, respectively, y_{CO_2} is the mole fraction of CO_2 in the gas phase, and n_{CO_2} and n^t_{amine} are the total moles of carbon dioxide and amine loaded into the equilibrium cell, respectively. The molar density of the vapor phase was calculated using the PR EoS.[57] The partial pressure of solvent in the gas phase was assumed to be equal to the vapor pressure of the solvent, $P^v_{solvent}$, at the equilibrium temperature. Thus, the mole fraction of CO_2 in the gas phase was calculated as[14]

$$y_{CO_2} = \frac{P_{CO_2}}{P_{eq}} = \frac{P_{eq} - P^v_{solvent}}{P_{eq}} \quad (2)$$

Additional amounts of CO_2 were metered into the cell, and the aforementioned procedure was followed for subsequent data points.

The method defined by National Institute of Standards and Technology (NIST) was followed to perform an uncertainty analysis.[58] The combined uncertainty can be determined using the law of propagation of uncertainty, as follows

https://dx.doi.org/10.1021/acs.jced.0c00618
J. Chem. Eng. Data 2021, 66, 899−914

Table 5. Experimental (exp) Data of the Solubility of CO_2 in Hybrid Solvent of MEA (1) + H_2O (2) + bmim[OTF] (3) with Different Initial Mass Composition (w), Including the Measured Temperature (T), Pressure (P), Volume of Gas Phase (V_g), Total Number of Moles of Solvent ($n_{solvent}$), Number of Moles of CO_2 (n_{CO_2}), Total Mole Fraction of CO_2 (z_{CO_2}), Apparent Mole Fraction of CO_2 in Liquid Phase[a] (x_{CO_2}), and Solubility of CO_2[b] (a_{CO_2}), Including the Expanded Uncertainties (k = 2), $U(T)$ = 0.02 K, $U(P)$ = 0.002 MPa, and $U(w)$ = 0.0001

T (K)	P(MPa)	V_g(cm^3)	n_{CO_2} (mol)	$n_{solvent}$ (mol)	z_{CO_2}	$U(z_{CO_2})$	$x^{exp}_{CO_2}$	$U(x_{CO_2})$	$a^{exp}_{CO_2}$	$U(a_{CO_2})$
				$w_1/w_2/w_3$ = 0.2980/0.6017/0.1003						
313.14	0.406	14.74	0.0757	0.8293	0.0836	0.0008	0.0813	0.0008	0.7004	0.0072
313.12	1.089	14.58	0.0898	0.8293	0.0977	0.0008	0.0913	0.0009	0.7957	0.0082
313.11	1.473	14.55	0.0958	0.8293	0.1035	0.0010	0.0949	0.0011	0.8298	0.0102
313.12	1.910	14.46	0.1020	0.8293	0.1095	0.0012	0.0983	0.0012	0.8625	0.0120
313.10	2.206	14.43	0.1060	0.8293	0.1133	0.0017	0.1002	0.0018	0.8814	0.0175
298.08	0.215	14.90	0.0757	0.8293	0.0836	0.0008	0.0823	0.0008	0.7101	0.0074
298.05	0.676	14.73	0.0898	0.8293	0.0977	0.0008	0.0936	0.0008	0.8171	0.0081
298.08	0.960	14.67	0.0958	0.8293	0.1035	0.0010	0.0977	0.0011	0.8569	0.0103
298.08	1.310	14.61	0.1020	0.8293	0.1095	0.0012	0.1015	0.0012	0.8944	0.0118
298.05	1.554	14.53	0.1060	0.8293	0.1133	0.0017	0.1038	0.0018	0.9167	0.0175
				$w_1/w_2/w_3$ = 0.2994/0.4614/0.2392						
313.08	0.448	14.41	0.0779	0.7106	0.0988	0.0010	0.0959	0.0010	0.6782	0.0080
313.09	1.081	14.17	0.0920	0.7106	0.1146	0.0011	0.1077	0.0011	0.7717	0.0087
313.09	1.389	14.14	0.0971	0.7106	0.1203	0.0012	0.1114	0.0012	0.8014	0.0099
313.09	1.780	14.01	0.1034	0.7106	0.1271	0.0013	0.1157	0.0014	0.8362	0.0110
313.10	2.171	13.96	0.1092	0.7106	0.1332	0.0018	0.1192	0.0019	0.8653	0.0156
298.03	0.232	14.60	0.0779	0.7106	0.0988	0.0010	0.0972	0.0010	0.6884	0.0081
298.02	0.672	14.36	0.0920	0.7106	0.1146	0.0010	0.1101	0.0011	0.7910	0.0085
298.05	0.889	14.24	0.0971	0.7106	0.1203	0.0012	0.1144	0.0012	0.8256	0.0100
298.03	1.200	14.15	0.1034	0.7106	0.1271	0.0013	0.1191	0.0013	0.8644	0.0108
298.04	1.509	14.04	0.1092	0.7106	0.1332	0.0018	0.1232	0.0019	0.8982	0.0156
				$w_1/w_2/w_3$ = 0.2924/0.3071/0.4005						
313.12	0.540	14.57	0.0764	0.5371	0.1245	0.0011	0.1201	0.0011	0.6619	0.0071
313.12	1.142	14.33	0.0893	0.5371	0.1426	0.0012	0.1334	0.0012	0.7466	0.0078
313.13	1.362	14.29	0.0932	0.5371	0.1479	0.0013	0.1370	0.0014	0.7697	0.0089
313.11	1.727	14.17	0.0995	0.5371	0.1563	0.0014	0.1425	0.0015	0.8058	0.0099
313.11	2.036	14.09	0.1045	0.5371	0.1629	0.0020	0.1467	0.0021	0.8335	0.0142
298.06	0.290	14.77	0.0764	0.5371	0.1245	0.0011	0.1220	0.0012	0.6739	0.0072
298.06	0.742	14.53	0.0893	0.5371	0.1426	0.0012	0.1364	0.0012	0.7655	0.0076
298.04	0.901	14.45	0.0932	0.5371	0.1479	0.0013	0.1404	0.0014	0.7918	0.0090
298.05	1.189	14.35	0.0995	0.5371	0.1563	0.0014	0.1464	0.0015	0.8317	0.0098
298.07	1.426	14.24	0.1045	0.5371	0.1629	0.0021	0.1511	0.0021	0.8634	0.0143

[a] $x_{CO_2} = \frac{n^L_{CO_2}}{n^L_{CO_2} + n_{solvent}}$. [b] $a_{CO_2} = \frac{n^L_{CO_2}}{n^t_{amine}}$.

$$u_c^2(y) = \sum_{i=1}^{N} \left(\frac{\partial f}{\partial x_i}\right)^2 u_c^2(x_i) + 2\sum_{i=1}^{N-1}\sum_{j=i+1}^{N} \frac{\partial f}{\partial x_i}\frac{\partial f}{\partial x_j} u(x_i, x_j) \quad (3)$$

where f is a measurement equation between the output result (y) and the measured inputs (x) in the form of $y = f(x_1, x_2,..., x_N)$. The estimates used to calculate the uncertainty are listed in Table 2. Expanded uncertainties for temperature, pressure, and solubility of CO_2 were determined using a coverage factor of k = 2.

3. DATA MODELING

The data measured for viscosity, density, and sound velocity were fitted to the Vogel−Fulcher−Tammann (VFT), quadratic, and linear equations, respectively[56,59−61]

$$\eta = A_1 \exp\left[\frac{A_2}{T - A_3}\right] \quad (4)$$

$$\rho = B_1 T^2 + B_2 T + B_3 \quad (5)$$

$$c = D_1 T + D_2 \quad (6)$$

where η(mPa·s), ρ(g/cm^3), c(m/s), and T(K) are viscosity, density, sound velocity, and temperature, and A, B, and D are fitting parameters.

4. RESULTS AND DISCUSSION

Table 3 lists an overview of the solvents synthesized of MEA + bmim[OTF] + H_2O and MEA + bmim[TF_2N] + NMP solutions used for the measurement of CO_2 solubility, viscosity, density, sound velocity, and evaporation rates used in this work.

4.1. Solubility Measurements. *4.1.1. MEA + H_2O + bmim[OTF] Solutions.* In this section, we investigate the addition of an IL (bmim[OTF]) to an aqueous MEA solvent. The solubilities of CO_2 in mixtures of (MEA + H_2O) and (MEA + H_2O + bmim[OTF]) at temperatures of 313.15 and 298.15 K were experimentally measured. The measured data

https://dx.doi.org/10.1021/acs.jced.0c00618
J. Chem. Eng. Data 2021, 66, 899−914

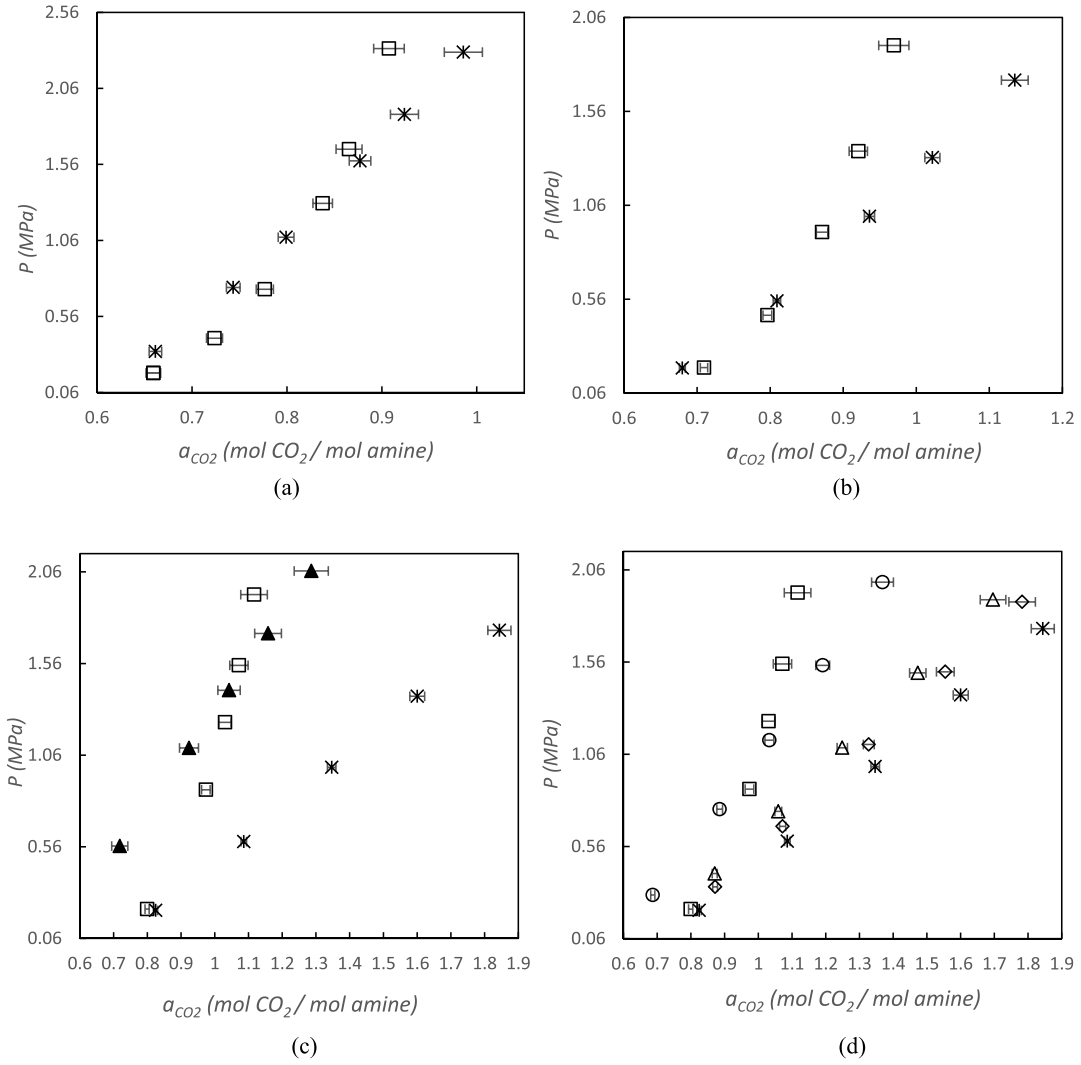

Figure 2. Comparison of experimental data for the solubility of CO_2 in: (a) MEA (1) +H_2O (2) with mass composition of w_1/w_2 = 0. 2965/0.7034 (□), and MEA (1) + NMP (2) with w_1/w_2 = 0.3037/0.6963 (*); (b) MEA (1) + H_2O (2) with w_1/w_2 = 0.1997/0.8003 (□); and MEA (1) + NMP (2) with w_1/w_2 = 0.2032/0.7968 (*); (c) MEA (1) + H_2O (2) with w_1/w_2 = 0.1034/0.8966 (□), MEA (1) + NMP (2) with w_1/w_2 = 0.1025/0.8975 (*), and MEA (1) + bmim[OTF] (2) with w_1/w_2 = 0.0912/0.9088 (▲); and (d) MEA (1) + H_2O (2) with w_1/w_2 = 0.1034/0.8966 (□), MEA (1) + NMP (2) with of w_1/w_2 = 0.1025/0.8975 (*), and MEA (1) + NMP (2) + bmim[TF_2N] (3) with different mass compositions: $w_1/w_2/w_3$ = 0.1039/0.7966/0.0995 (◇), $w_1/w_2/w_3$ = 0.0977/0.6492/0.2531 (△), and $w_1/w_2/w_3$ = 0.1162/0.4932/0.3906 (○), at 313.15 K.

are displayed in Figure 1 and listed in Tables 4 and 5. The initial concentration of amine in the solvent mixture was maintained relatively consistent to enable comparison between solubility of CO_2 (a_{CO_2} = total moles of CO_2 absorbed in the liquid phase/initial moles of amine) in various solvents. From Figure 1, it is evident that the presence of bmim[OTF] in the 30 wt % MEA aqueous solution decreases the solubility of CO_2. Compared to the 29.65 wt% MEA aqueous solution at 298.15 and 313.15 K and pressure range of 0.1−2 MPa, the solubility of CO_2 in the hybrid MEA solvents, with an approximate mass fraction of 0.30 of the MEA and mass fractions of 0.1003, 0.2392, and 0.4005 of the IL, decreases by approximately 0.5−4.5%, 2.5−7%, and 5−11.5%, respectively. However, in commercial processes due to corrosion issues, the allowable acid gas loading in the amine solutions is limited. Thus, the maximum loading for MEA solutions is usually between 0.3−0.35 and 0.7−0.9 (moles of acid gas/mole of MEA) for carbon steel and stainless steel equipment, respectively.[51−54] It is prudent to note that the maximum loading of acid gas in the amine solvent can be controlled through many tower parameters, for example, pressure, number of trays, and solvent flow. Thus, a higher solubility of acid gas in the solvent is always preferred. It is clear from the measured data that all of the studied hybrid MEA solvents are able to achieve the maximum allowable loading of the acid gas even at moderate pressures. However, the tray requirements of an absorption column may increase due to the decrease in both the solubility of carbon dioxide and tray efficiency.

4.1.2. MEA + H_2O, MEA + bmim[OTF] and MEA + NMP + bmim[TF_2N] Solutions. Rivas and Prausnitz have previously reported on the potential benefits relating to the addition of NMP to chemical solvents for the bulk removal of acid gases.[62] Therefore, in this section, considering the aqueous MEA solvent, we ultimately investigate the replacement of the aqueous phase of the solvent with NMP, bmim[OTF], and/or bmim[TF_2N]. The solubility of CO_2 in mixtures of MEA + H_2O, MEA + bmim[OTF] and MEA + NMP + bmim[TF_2N], with different concentrations of MEA, viz., $w \sim$ (0.1, 0.2, and 0.3), as listed in Table 3, was measured at 313.15 K. Water was

https://dx.doi.org/10.1021/acs.jced.0c00618
J. Chem. Eng. Data 2021, 66, 899−914

Table 6. Experimental (exp) Data for the Solubility of CO_2 in the Hybrid Solvent of MEA (1) + NMP (2) with Different Initial Mass Compositions (w), Including the Measured Temperature (T), Pressure (P), Volume of Gas Phase (V_g), Total Number of Moles of Solvent ($n_{solvent}$), Number of Moles of CO_2 (n_{CO_2}), Total Mole Fraction of CO_2 (z_{CO_2}), Apparent Mole Fraction of CO_2 in Liquid Phase[a] (x_{CO_2}), and Solubility of CO_2[b] (a_{CO_2}), Including the Expanded Uncertainties (k = 2), $U(T)$ = 0.02 K, $U(P)$ = 0.002 MPa, and $U(w)$ = 0.0001

T (K)	P(MPa)	V_g(cm^3)	n_{CO_2} (mol)	$n_{solvent}$ (mol)	z_{CO_2}	$U(z_{CO_2})$	$x^{exp}_{CO_2}$	$U(x_{CO_2})$	$a^{exp}_{CO_2}$	$U(a_{CO_2})$
				w_1/w_2 = 0.3037/0.6963						
313.034	0.330	14.41	0.0718	0.2550	0.2196	0.0017	0.2151	0.0017	0.6614	0.0066
313.039	0.751	14.11	0.0828	0.2550	0.2451	0.0017	0.2355	0.0017	0.7434	0.0072
313.032	1.081	13.88	0.0905	0.2550	0.2620	0.0019	0.2488	0.0019	0.7991	0.0083
313.076	1.583	13.62	0.1017	0.2550	0.2850	0.0024	0.2666	0.0025	0.8770	0.0113
313.065	1.889	13.42	0.1084	0.2550	0.2982	0.0030	0.2768	0.0032	0.9238	0.0148
313.084	2.298	13.19	0.1173	0.2550	0.3151	0.0039	0.2901	0.0042	0.9859	0.0201
				w_1/w_2 = 0.2032/0.7968						
313.04	0.194	14.56	0.0494	0.2428	0.1691	0.0008	0.1660	0.0008	0.6798	0.0041
313.05	0.551	14.28	0.0606	0.2428	0.1998	0.0009	0.1915	0.0010	0.8093	0.0051
313.04	1.001	13.93	0.0722	0.2428	0.2291	0.0012	0.2151	0.0013	0.9360	0.0070
313.07	1.314	13.69	0.0800	0.2428	0.2479	0.0017	0.2303	0.0018	1.0221	0.0104
313.00	1.726	13.39	0.0904	0.2428	0.2712	0.0028	0.2494	0.0030	1.1348	0.0183
				w_1/w_2 = 0.1025/0.8975						
313.04	0.213	15.07	0.0309	0.2304	0.1184	0.0007	0.1142	0.0007	0.8247	0.0059
313.10	0.588	14.30	0.0424	0.2304	0.1555	0.0009	0.1451	0.0009	1.0860	0.0082
313.08	0.993	13.92	0.0541	0.2304	0.1901	0.0013	0.1739	0.0013	1.3467	0.0126
313.06	1.381	13.52	0.0653	0.2304	0.2209	0.0021	0.2001	0.0022	1.6003	0.0222
313.05	1.741	13.18	0.0760	0.2304	0.2481	0.0030	0.2237	0.0032	1.8438	0.0342

[a] $x_{CO_2} = \frac{n^{L}_{CO_2}}{n^{L}_{CO_2} + n_{solvent}}$. [b] $a_{CO_2} = \frac{n^{L}_{CO_2}}{n^{t}_{amine}}$.

Table 7. Experimental (exp) Data for the Solubility of CO_2 in Hybrid Solvent of MEA (1) + H_2O (2) with Different Initial Mass Composition (w), Including the Measured Temperature (T), Pressure (P), Volume of Gas Phase (V_g), Total Number of Moles of Solvent ($n_{solvent}$), Number of Moles of CO_2 (n_{CO_2}), Total Mole Fraction of CO_2 (z_{CO_2}), Apparent Mole Fraction of CO_2 in Liquid Phase[a] (x_{CO_2}), and Solubility of CO_2[b] (a_{CO_2}), Including the Expanded Uncertainties (k = 2), $U(T)$ = 0.02 K, $U(P)$ = 0.002 MPa, and $U(w)$ = 0.0001

T (K)	P(MPa)	V_g(cm^3)	n_{CO_2} (mol)	$n_{solvent}$ (mol)	z_{CO_2}	$U(z_{CO_2})$	$x^{exp}_{CO_2}$	$U(x_{CO_2})$	$a^{exp}_{CO_2}$	$U(a_{CO_2})$
				w_1/w_2 = 0.1997/0.8003						
312.99	0.196	15.44	0.0486	0.9764	0.0474	0.0003	0.0464	0.0003	0.7095	0.0050
313.04	0.475	15.40	0.0561	0.9764	0.0544	0.0004	0.0518	0.0004	0.7962	0.0060
313.03	0.917	15.30	0.0639	0.9764	0.0614	0.0005	0.0564	0.0005	0.8711	0.0079
313.01	1.348	15.22	0.0700	0.9764	0.0669	0.0007	0.0594	0.0008	0.9207	0.0125
312.99	1.911	15.18	0.0771	0.9764	0.0732	0.0012	0.0623	0.0012	0.9693	0.0207
				w_1/w_2 = 0.1034/0.8966						
313.04	0.220	15.70	0.0295	1.0718	0.0268	0.0002	0.0256	0.0002	0.7994	0.0062
313.01	0.871	15.59	0.0397	1.0718	0.0357	0.0004	0.0310	0.0004	0.9737	0.0127
313.06	1.239	15.56	0.0442	1.0718	0.0396	0.0005	0.0328	0.0006	1.0303	0.0183
313.03	1.550	15.51	0.0477	1.0718	0.0426	0.0008	0.0341	0.0008	1.0716	0.0271
313.01	1.936	15.51	0.0521	1.0718	0.0463	0.0012	0.0354	0.0012	1.1165	0.0395

[a] $x_{CO_2} = \frac{n^{L}_{CO_2}}{n^{L}_{CO_2} + n_{solvent}}$. [b] $a_{CO_2} = \frac{n^{L}_{CO_2}}{n^{t}_{amine}}$.

also replaced such that the systems of CO_2 + MEA + NMP and CO_2 + MEA + bmim[OTF] at a temperature of 313.15 K were measured. Finally, the inclusion of different concentrations of bmim[TF_2N] in the NMP-containing 10% MEA solution was studied at a temperature of 313.15 K.

The data are presented in Figure 2 and listed in Tables 6−9. Figure 2a−c compares the solubility of CO_2 in an MEA aqueous solution with a water-free NMP-containing MEA solution at a temperature of 313.15 K. It is evident from the figures that there is a turning point or a pressure point for each set of measurements. It is dependent on the initial concentration of MEA and decreases with reducing concentration of MEA. The turning point for the CO_2 + MEA + H_2O and CO_2 + MEA + NMP ternary systems ($w_{MEA} \sim 0.3$), displayed in Figure 2a, is approximately 1.4 MPa. The results show that the solubility of CO_2 in the 29.6 wt % MEA aqueous solution is approximately 5.5% higher compared to the 30.4 wt % MEA + NMP solution within the pressure range of 0.3−1.4 MPa. Furthermore, the substitution of water with NMP in the CO_2 + MEA systems increases the CO_2 solubility by a maximum of 6.5% within the pressure range of 1.4−2 MPa. As displayed in Figure 2b, the turning point for the CO_2 + MEA +

https://dx.doi.org/10.1021/acs.jced.0c00618
J. Chem. Eng. Data 2021, 66, 899−914

Table 8. Experimental (exp) Data for the Solubility of CO_2 in Hybrid Solvent of MEA (1) + bmim[OTF] (2) with w_1/w_2 = 0.0912/0.9088, Including the Measured Temperature (T), Pressure (P), Volume of Gas Phase (V_g), Total Number of Moles of Solvent ($n_{solvent}$), Number of Moles of CO_2 (n_{CO_2}), Total Mole Fraction of CO_2 (z_{CO_2}), Apparent Mole Fraction of CO_2 in Liquid Phase[a] (x_{CO_2}), and Solubility of CO_2[b] (a_{CO_2}), Including the Expanded Uncertainties (k = 2), $U(T)$ = 0.02 K, $U(P)$ = 0.002 MPa, and $U(w)$ = 0.0001

T (K)	P(MPa)	V_g(cm^3)	n_{CO_2} (mol)	$n_{solvent}$ (mol)	z_{CO_2}	$U(z_{CO_2})$	$x^{exp}_{CO_2}$	$U(x_{CO_2})$	$a^{exp}_{CO_2}$	$U(a_{CO_2})$
313.04	0.564	15.18	0.0310	0.1198	0.2057	0.0048	0.1875	0.0050	0.7183	0.0238
313.03	1.099	14.90	0.0422	0.1198	0.2605	0.0049	0.2288	0.0054	0.9235	0.0282
313.00	1.414	14.73	0.0487	0.1198	0.2891	0.0054	0.2509	0.0060	1.0423	0.0332
313.02	1.724	14.56	0.0551	0.1198	0.3151	0.0060	0.2712	0.0068	1.1579	0.0397
313.01	2.065	14.40	0.0622	0.1198	0.3419	0.0070	0.2924	0.0081	1.2861	0.0505

[a] $x_{CO_2} = \frac{n^L_{CO_2}}{n^L_{CO_2} + n_{solvent}}$. [b] $a_{CO_2} = \frac{n^L_{CO_2}}{n^t_{amine}}$.

Table 9. Experimental (exp) Data for the Solubility of CO_2 in Hybrid Solvent of MEA (1) + NMP (2) + bmim[TF_2N] (3) with Different Initial Mass Compositions (w), Including the Measured Temperature (T), Pressure (P), Volume of Gas Phase (V_g), Total Number of Moles of Solvent ($n_{solvent}$), Number of Moles of CO_2 (n_{CO_2}), Total Mole Fraction of CO_2 (z_{CO_2}), Apparent Mole Fraction of CO_2 in Liquid Phase[a] (x_{CO_2}), and Solubility of CO_2[b] (a_{CO_2}), Including the Expanded Uncertainties (k = 2), $U(T)$ = 0.02 K, $U(P)$ = 0.002 MPa, and $U(w)$ = 0.0001

T (K)	P(MPa)	V_g(cm^3)	n_{CO_2} (mol)	$n_{solvent}$ (mol)	z_{CO_2}	$U(z_{CO_2})$	$x^{exp}_{CO_2}$	$U(x_{CO_2})$	$a^{exp}_{CO_2}$	$U(a_{CO_2})$
				$w_1/w_2/w_3$ = 0.1039/0.7966/0.0995						
313.09	0.341	14.46	0.0349	0.2215	0.1360	0.0009	0.1294	0.0009	0.8719	0.0070
313.10	0.669	14.17	0.0443	0.2215	0.1665	0.0011	0.1546	0.0011	1.0720	0.0092
313.09	1.113	13.81	0.0564	0.2215	0.2029	0.0017	0.1846	0.0018	1.3275	0.0160
313.06	1.507	13.48	0.0672	0.2215	0.2326	0.0026	0.2096	0.0028	1.5547	0.0263
313.05	1.886	13.08	0.0778	0.2215	0.2599	0.0037	0.2331	0.0039	1.7827	0.0393
				$w_1/w_2/w_3$ = 0.0977/0.6492/0.2531						
313.05	0.413	14.87	0.0343	0.2002	0.1461	0.0010	0.1373	0.0010	0.8705	0.0075
313.05	0.750	14.60	0.0431	0.2002	0.1772	0.0012	0.1622	0.0013	1.0591	0.0102
313.04	1.095	14.36	0.0521	0.2002	0.2064	0.0017	0.1858	0.0018	1.2490	0.0152
313.07	1.501	13.99	0.0626	0.2002	0.2382	0.0025	0.2121	0.0027	1.4730	0.0242
313.05	1.898	13.67	0.0730	0.2002	0.2674	0.0037	0.2366	0.0040	1.6961	0.0380
				$w_1/w_2/w_3$ = 0.1162/0.4932/0.3906						
313.01	0.297	15.71	0.0322	0.1817	0.1506	0.0011	0.1433	0.0011	0.6869	0.0061
313.00	0.762	15.38	0.0439	0.1817	0.1944	0.0013	0.1774	0.0014	0.8853	0.0084
313.04	1.136	15.14	0.0527	0.1817	0.2249	0.0019	0.2010	0.0021	1.0328	0.0132
313.03	1.542	14.87	0.0622	0.1817	0.2552	0.0027	0.2249	0.0030	1.1911	0.0205
313.01	1.993	14.63	0.0730	0.1817	0.2866	0.0040	0.2500	0.0044	1.3683	0.0324

[a] $x_{CO_2} = \frac{n^L_{CO_2}}{n^L_{CO_2} + n_{solvent}}$. [b] $a_{CO_2} = \frac{n^L_{CO_2}}{n^t_{amine}}$.

H_2O and CO_2 + MEA + NMP ternary systems ($w_{MEA} \sim 0.2$) is approximately 0.6 MPa. For these ternary systems, CO_2 exhibits a higher solubility (around 4.5% higher) in the aqueous solvent within the pressure range of 0.2−0.6 MPa. However, at pressures between 0.6 and 2 MPa, the replacement of water with NMP increases the CO_2 solubility by a maximum of 25%. Finally, the turning point for the CO_2 + MEA + H_2O and CO_2 + MEA + NMP ternary systems ($w_{MEA} \sim 0.1$), shown in Figure 2c, is approximately 0.2 MPa (more data at lower pressures are required to obtain the turning point more accurately). The data show that the replacement of water with NMP in the 10.34 wt % MEA aqueous solution increases the CO_2 solubility significantly by almost 81% at pressures between 0.213 and 2 MPa. Additionally, Figure 2c shows the solubility of CO_2 in the water-free bmim[OTF]-containing MEA solution. It is clear from the figure that bmim[OTF] does not improve the ability of the MEA solution to absorb CO_2 at lower pressures. In this case, the turning point for the CO_2 + MEA + H_2O and CO_2 + MEA + bmim[OTF] ternary systems ($w_{MEA} \sim 0.1$) is approximately 1.5 MPa. At pressures above the turning point, the replacement of water with bmim[OTF] increases the solubility of CO_2 by a maximum of 12% at pressures between 1.5 and 2 MPa. Figure 2d displays solubility data for the CO_2 + MEA + H_2O and CO_2 + MEA + NMP ternary systems ($w_{MEA} \sim 0.1$) as well as the CO_2 + MEA + bmim[TF_2N] + NMP quaternary system ($w_{MEA} \sim 0.1$). In this case, replacement of aqueous media with a mixture of bmim[TF_2N] (w = 0.0995) + NMP in the 10 wt % MEA aqueous solution increases the CO_2 solubility by a maximum of 65% at pressures between 0.341 and 2 MPa. In summary, regarding only the solubility of CO_2, at pressures above 1.1 MPa, the mixed ternary solvents presented herein all outperform the aqueous MEA solvent. However, the addition of the ILs in either case does not outperform the MEA + NMP solvent ($w_{MEA} \sim 0.1$). Compared to the NMP-containing 10.25 wt % MEA solution at 313.15 K and pressure range of 0.4−2 MPa, the solubility of CO_2 in the hybrid solvents of NMP + MEA + bmim[TF_2N], with an approximate mass fraction of

https://dx.doi.org/10.1021/acs.jced.0c00618
J. Chem. Eng. Data 2021, 66, 899−914

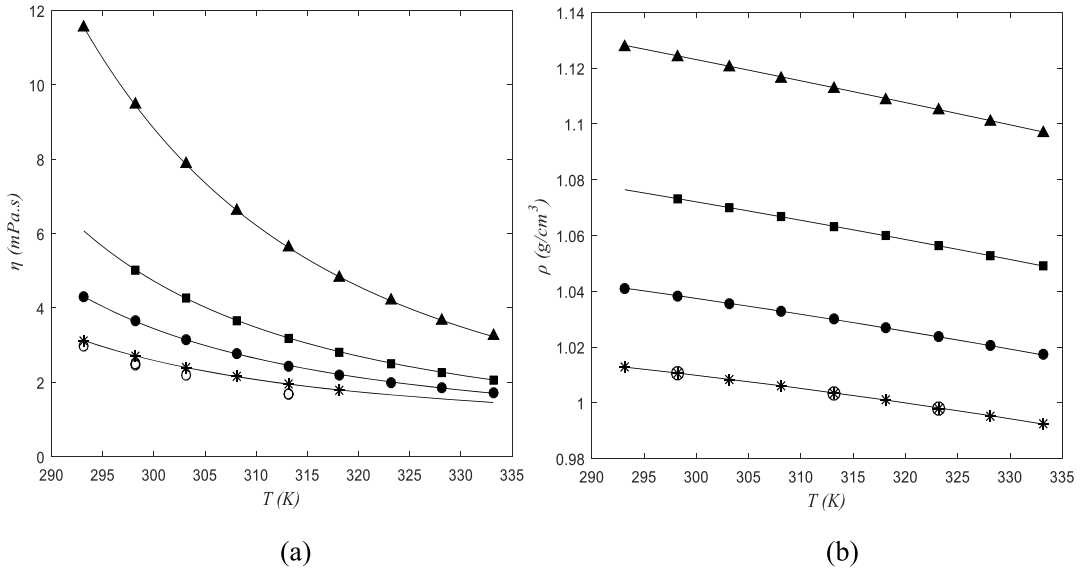

Figure 3. (a) Viscosity (relative expanded uncertainty of $U_r(\eta)$ = 0.004) and (b) density (relative expanded uncertainty of $U_r(\rho)$ = 0.004) versus temperature for mixtures of MEA (1) + H_2O (2) + bmim[OTF] (3) with different mass compositions: Exp (this work) w_2/w_1 = 0.6996/0.3004 (*), $w_3/w_2/w_1$ = 0.1045/0.5836/0.3119 (●), $w_3/w_2/w_1$ = 0.2392/0.4614/0.2994 (■), and $w_3/w_2/w_1$ = 0.4311/0.2643/0.3046 (▲); literature data w_2/w_1 = 0.7/0.3 (○).[64,65] The solid line depicts regressed results.

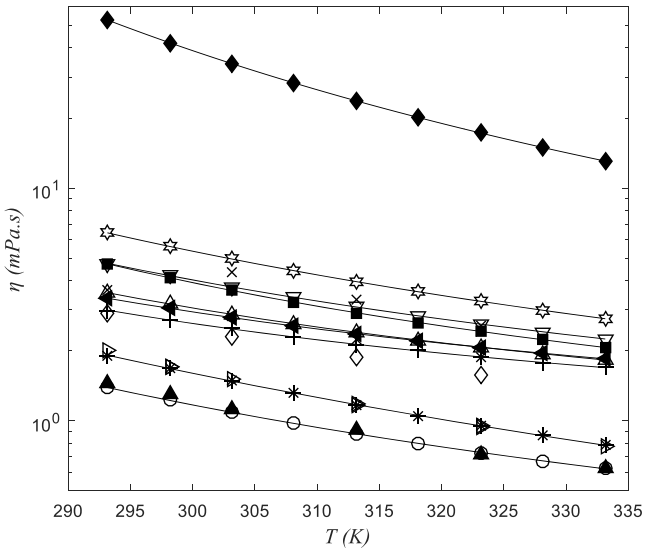

Figure 4. Viscosity (relative expanded uncertainty of $U_r(\eta)$ = 0.004) versus temperature for mixtures of MEA (1) + NMP (2) + bmim[TF_2N] (3) with different mass compositions: w_1/w_2 = 0.1021/0.8979 (+), w_1/w_2 = 0.2090/0.7910 (△), w_1/w_2 = 0.3089/0.6911 (■), $w_1/w_2/w_3$ = 0.0976/0.8032/0.0992 (◀), $w_1/w_2/w_3$ = 0.1138/0.6414/0.2448 (▽), $w_1/w_2/w_3$ = 0.1162/0.4932/0.3906 (☆); MEA (1) + bmim[OTF] (2) with mass fraction w_1/w_2 = 0.0912/0.9088 (♦); and mixtures of MEA (1) + H_2O (2) with mass fractions: w_1/w_2 = 0.1034/0.8966 (○) and w_1/w_2 = 0.2008/0.7992 (*). The solid line depicts regressed results. Literature data for: MEA (1) + H_2O (2), w_1 = 0.1000 (▲),[65] w_1 = 0.2000 (▷);[64,65] MEA (1) + NMP (2), w_1 = 0.2089 (◇),[66] w_1 ≈ 0.30 (×).[66,67]

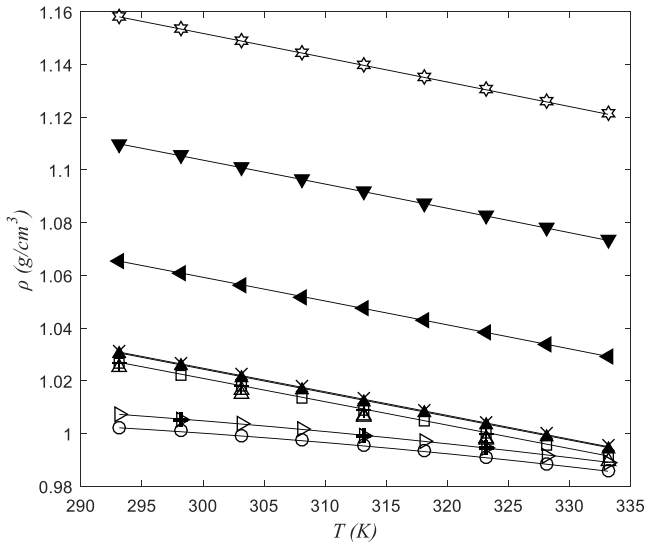

Figure 5. Density (relative expanded uncertainty of $U_r(\rho)$ = 0.004) versus temperature for mixtures of MEA (1) + NMP (2) + bmim[TF_2N] (3) mixtures with different mass compositions: w_1/w_2 = 0.1025/0.8975 (×), w_1/w_2 = 0.199/0.801 (▲), w_1/w_2 = 0.3074/0.6926 (□), $w_1/w_2/w_3$ = 0.0976/0.8032/0.0992 (◀), $w_1/w_2/w_3$ = 0.1138/0.6414/0.2448 (▼), $w_1/w_2/w_3$ = 0.1162/0.4932/0.3906 (☆); mixtures of MEA (1) + H_2O (2) with mass fractions: w_1/w_2 = 0.1034/0.8966 (○), w_1/w_2 = 0.2008/0.7992 (▷). The solid line depicts regressed results. Literature data for: MEA (1) + H_2O (2), w_1 = 0.2000 (bold +);[64] MEA (1) + NMP (2), w_1 = 0.2089 (+),[66] w_1 ≈ 0.30 (△).[66,67]

0.10 of the MEA and mass fractions of 0.0995, 0.2531, and 0.3906 of the IL, decreases approximately by 5−9%, 10−14%, and 23.5−33%, respectively. On the contrary, the existence of the turning point may be beneficial for the solvent regeneration column. In all cases, at low pressures, the addition of the IL and NMP to the mixed solvents exhibits a lower solubility of carbon dioxide compared to the aqueous MEA solvent. Thus, we can expect improved efficiency for regeneration that occurs at low pressures.

4.2. Viscosity, Density, and Speed of Sound Measurements. Viscosity, density, and sound velocity data for the mixtures listed in Table 3 were measured. The mixtures include the binary system of MEA + NMP, MEA + bmim[OTF], MEA + H_2O, and ternary mixtures of MEA + H_2O + bmim[OTF] and MEA + NMP + bmim[TF_2N]. The

https://dx.doi.org/10.1021/acs.jced.0c00618
J. Chem. Eng. Data 2021, 66, 899−914

Table 10. Data of the Viscosity (η), Density (ρ), and Sound Velocity (c) at Different Mass Compositions (w) for the System of MEA (1) + H_2O (2) + bmim[OTF] (3)[a]

	temperature (K)								
property	293.15	298.15	303.15	308.15	313.15	318.15	323.15	328.15	333.15
				w_1/w_2 = 0.3004/0.6996					
η (mPa·s)	3.125	2.714	2.397	2.143	1.950	1.795			
	2.990[b]	2.48[b]	2.195[b]		1.67[b]				
		2.489[b]			1.671[b]				
ρ (g/cm^3)	1.013	1.011	1.008	1.006	1.003	1.001	0.998	0.995	0.992
		1.0106[b]			1.0034[b]		0.9981[b]		
c (m/s)	1672.7	1672.6	1671.6	1669.8	1667.3	1664.0	1659.8	1655.2	1649.8
				$w_1/w_2/w_3$ = 0.3119/0.5836/0.1045					
η (mPa·s)	4.300	3.656	3.152	2.758	2.447	2.198	2.004	1.847	1.718
ρ (g/cm^3)	1.041	1.039	1.036	1.033	1.030	1.027	1.024	1.021	1.017
c (m/s)	1701.8	1696.6	1691.0	1685.0	1678.5	1671.7	1664.3	1656.4	1648.0
				$w_1/w_2/w_3$ = 0.2994/0.4614/0.2392					
η (mPa·s)		5.025	4.267	3.670	3.186	2.805	2.511	2.269	2.073
ρ (g/cm^3)		1.073	1.070	1.067	1.063	1.060	1.056	1.053	1.049
c (m/s)		1685.7	1677.4	1668.9	1659.9	1650.7	1641.1	1631.2	1621.2
				$w_1/w_2/w_3$ = 0.3046/0.2643/0.4311					
η (mPa·s)	11.545	9.477	7.866	6.611	5.618	4.823	4.182	3.665	3.242
ρ (g/cm^3)	1.128	1.124	1.120	1.116	1.113	1.109	1.105	1.101	1.097
c (m/s)	1651.0	1640.3	1629.3	1618.2	1606.8	1595.3	1583.6	1571.6	1559.5

[a]Expanded uncertainties are: $U(w)$ = 0.0001, $U(T)$ = 0.02 K, $U_r(\rho)$ = 0.004, $U_r(\eta)$ = 0.004, and $U(c)$ = 0.7 m·s^{-1} (Data recorded at 0.101 MPa, $U(P)$ = 0.001 MPa). [b]Literature data for the viscosity and density of binary system of MEA (1) + H_2O (2), w_1 = 0.3000.[64,65]

experimental data are presented in Figures 3, 4, and 5 and listed in Tables 10 and 11. The fitted parameters and statistical deviations are listed in Tables 12 and 13. Furthermore, deviations between the experimental and literature density data are graphically compared in Figure 6. Considering all systems and temperatures, the maximum deviation between the experimental density and data available in the literature is 0.0035 g/cm^3. Figure 4 shows that the use of an IL instead of water considerably increases the viscosity in MEA solutions. The viscosity of the water-free bmim[OTF]-containing 9.12 wt % MEA solution is greater than the viscosity of the 10.34 wt % MEA aqueous solution by a factor of 21−38.1, over the entire range of temperatures investigated. However, the replacement of the aqueous media with NMP in the MEA aqueous solutions with different mass fractions of MEA, viz., ∼0.1, 0.2, and 0.3, increases the viscosity by a maximum factor of 2.6. The addition of IL to an aqueous/nonaqueous MEA solution increases the viscosity. For instance, the addition of bmim[TF_2N] to the NMP solution containing 10.21 wt % MEA to make a mixture of bmim[TF_2N] and MEA with mass fractions of 0.3906 and 0.1162, respectively, increases the viscosity by a factor of 1.6−2.1. In every case, the adjustment to the aqueous MEA solvent results in an increased viscosity. The increased viscosity may result in decreased tray efficiencies in the absorption/regeneration columns and may counteract the increased CO_2 solubility.

4.3. Evaporation Rate Measurements. The evaporation rates of samples listed in Table 3 were measured. Figures 7−9 display the sample mass versus time at 373.15 K. The evaporation rate is dependent on many physical properties, for example, the energy added to the system, pressure, surface area, etc. The binary mixture of water + MEA has been noted in the literature to be zeotropic.[63] Furthermore, water is far more volatile than MEA; given that the evaporation rates were determined at 373.15 K, it was assumed that the majority of the water content would evaporate prior to the evaporation of MEA. Based on this assumption, the individual evaporation rates of water and MEA were estimated. The experimental and estimated data are listed in Tables 14 and 15. Figure 7 shows that the 30.04 wt % MEA aqueous solution had evaporated completely after 38 min, but the addition of bmim[OTF] to the 30.04 wt % MEA aqueous solution decreases the evaporation rate of MEA. The evaporation rate of MEA in the 31.19 wt % MEA aqueous solution with a 10.45 wt % IL is almost half of the evaporation rate of MEA in the IL-free 30.04 wt % MEA aqueous solution. It is clear from Figure 8 that replacing water with NMP in the MEA aqueous solutions with different concentrations of MEA decreases the evaporation rate of the samples. For instance, the evaporation rate of the NMP-containing 20.70 wt % MEA solution is approximately 58% of the evaporation rate of MEA in the 19.85 wt % MEA aqueous solution. Figure 9 and Table 15 show that the addition of bmim[TF_2N] to the NMP-containing 11.29 wt % MEA sample, to make solutions with 25.31 and 39.06% of the IL, decreases the average evaporation rate. Interestingly, the evaporation rate of MEA in the 9.12 wt % MEA solution with 90.88 wt % of bmim[OTF] is 9.85% of the evaporation rate of MEA in the 9.97 wt % MEA aqueous solution. Figures 7−9 show that the evaporation rate decreases with respect to time and becomes zero for the IL-containing samples after some time. Tables 14 and 15 show that the final mass of the IL-containing samples is approximately equal to the mass of IL present in the initial sample loaded in the TGA apparatus. Therefore, the loss of IL, the expensive portion of the hybrid solvent under conditions which are close to the desorption conditions (high temperature and low pressure) is practically zero. Hence, the addition of IL into the amine solutions not only decreases the volatile part of the solvent but also decelerates the evaporation rate of amine.

https://dx.doi.org/10.1021/acs.jced.0c00618
J. Chem. Eng. Data 2021, 66, 899−914

Table 11. Data of the Viscosity (η), Density (ρ), and Sound Velocity (c) at Different Mass Compositions (w) for the System of MEA (1) + H_2O (2)/bmim[OTF] (2)/(NMP (2) + bmim[TF_2N] (3))[a]

	temperature (K)								
property	293.15	298.15	303.15	308.15	313.15	318.15	323.15	328.15	333.15
				w_1 = 0.091, $w_{bmim[OTF]}$ = 0.9088					
η (mPa·s)	52.922	41.987	34.402	28.383	23.755	20.13	17.249	14.939	13.046
ρ (g/cm^3)	1.265	1.261	1.257	1.253	1.249	1.245	1.241	1.237	1.233
c (m/s)	1440.6	1428.8	1417.0	1405.2	1393.6	1382.1	1370.6	1359.2	1348.0
				w_1 = 0.1034, w_{water} = 0.8966					
η (mPa·s)	1.389	1.224	1.087	0.973	0.878	0.798	0.731	0.673	0.622
	1.442[b]	1.299[b]	1.121[b]		0.909[b]		0.715[b]		0.626[b]
ρ (g/cm^3)	1.002	1.001	0.999	0.998	0.996	0.993	0.991	0.989	0.986
		1.00074[b]	0.99913[b]		0.99537[b]				0.98585[b]
c (m/s)	1546.0	1555.2	1563.0	1569.4	1574.6	1578.6	1581.5	1583.4	1584.1
				w_1 = 0.1021, w_{NMP} = 0.8979					
η (mPa·s)	2.990	2.712	2.484	2.293	2.133	1.996	1.880	1.782	1.695
				w_1 = 0.1025, w_{NMP} = 0.8975					
ρ (g/cm^3)	1.031	1.027	1.022	1.018	1.013	1.009	1.004	1.000	0.995
c (m/s)	1578.1	1559.0	1539.7	1520.6	1501.5	1482.7	1464.0	1445.5	1427.2
				w_1 = 0.2008, w_{water} = 0.7992					
η (mPa·s)	1.903	1.689	1.482	1.310	1.168	1.048	0.948	0.863	0.789
	2.005[c]	1.70[c]	1.501[c]		1.18[c]		0.95[c]		0.775[c]
		1.702[c]			1.169[c]		0.945[c]		
ρ (g/cm^3)	1.007	1.005	1.004	1.001	0.999	0.997	0.994	0.992	0.989
		1.0053[c]			0.9991[c]		0.9943[c]		
c (m/s)	1609.0	1614.5	1618.4	1620.9	1622.3	1622.7	1622.0	1620.4	1617.9
				w_1 = 0.2090, w_{NMP} = 0.7910					
η (mPa·s)	3.547	3.176	2.869	2.612	2.397	2.218	2.065	1.938	1.830
	2.883[d]		2.296[d]		1.866[d]		1.574[d]		
				w_1 = 0.1990, w_{NMP} = 0.8010					
ρ (g/cm^3)	1.030	1.026	1.021	1.017	1.012	1.008	1.003	0.999	0.994
	1.02657[d]		1.018[d]		1.00869[d]		0.99974[d]		
c (m/s)	1591.9	1573.0	1553.9	1534.9	1516.1	1497.4	1478.8	1460.4	1442.4
	1587.7[d]		1549.8[d]		1512.1[d]		1474.5[d]		
				w_1 = 0.3089, w_{NMP} = 0.6911					
η (mPa·s)	4.720	4.121	3.633	3.236	2.909	2.638	2.415	2.228	2.075
	3.622[f]		4.361[e]		3.317[e]		2.559[e]		2.105[e]
			2.822[f]		2.245[f]		1.883[f]		
				w_1 = 0.3074, w_{NMP} = 0.6926					
ρ (g/cm^3)	1.027	1.022	1.018	1.013	1.009	1.005	1.000	0.996	0.991
	1.02491[f]		1.0147[e]		1.0062[e]		0.9977[e]		0.9892[e]
			1.0163[f]		1.0069[f]		0.99814[f]		
c (m/s)	1604.7	1586.1	1567.3	1548.6	1529.9	1511.4	1493.0	1474.8	1456.7
	1599.1[f]		1561.2[f]		1523.9[f]		1486.7[f]		
				w_1 = 0.0976, w_{NMP} = 0.8032, $w_{bmim[TF2N]}$ = 0.0992					
η (mPa·s)	3.357	3.042	2.776	2.553	2.364	2.204	2.068	1.950	1.848
ρ (g/cm^3)	1.065	1.061	1.056	1.052	1.047	1.043	1.038	1.034	1.029
c (m/s)	1553.8	1535.6	1517.2	1498.9	1480.9	1463.0	1445.3	1427.9	1410.8
				w_1 = 0.1138, w_{NMP} = 0.6414, $w_{bmim[TF2N]}$ = 0.2448					
η (mPa·s)	4.749	4.206	3.761	3.388	3.089	2.818	2.599	2.410	2.252
ρ (g/cm^3)	1.110	1.106	1.101	1.096	1.092	1.087	1.083	1.078	1.073
c (m/s)	1512.4	1495.3	1478.3	1461.3	1444.5	1427.8	1411.3	1395.1	1379.1
				w_1 = 0.1162, w_{NMP} = 0.4932, $w_{bmim[TF2N]}$ = 0.3906					
η (mPa·s)	6.416	5.617	4.959	4.413	3.958	3.575	3.254	2.982	2.752
ρ (g/cm^3)	1.158	1.154	1.149	1.145	1.140	1.135	1.131	1.126	1.121
c (m/s)	1463.2	1447.3	1431.4	1415.6	1399.9	1384.3	1368.8	1353.5	1338.4

[a]Expanded uncertainties are: $U(w)$ = 0.0001, $U(T)$ = 0.02 K, $U_r(\rho)$ = 0.004, $U_r(\eta)$ = 0.004, and $U(c)$ = 0.7 m·s^{-1} (Data recorded at 0.101 MPa, $U(P)$ = 0.001 MPa). [b]Literature data for the viscosity and density of the MEA (1) + H_2O (2) binary system ($w_1 \approx 0.1000$).[65,68] [c]Literature data for the viscosity and density of the MEA (1) + H_2O (2) binary system (w_1 = 0.2000).[64,65] [d]Literature data for the viscosity, density, and sound velocity for the MEA (1) + NMP (2) binary system (w_1 = 0.2089).[66] [e]Literature data for the viscosity and density for the MEA (1) + NMP (2) binary system (w_1 = 0.2917).[67] [f]Literature data for the viscosity, density, and sound velocity for the MEA (1) + NMP (2) binary system (w_1 = 0.2946).[66]

https://dx.doi.org/10.1021/acs.jced.0c00618
J. Chem. Eng. Data 2021, 66, 899−914

Table 12. Regressed Parameters and Statistical Deviations[a] (AAD) for Viscosity[b] (η), Density[c] (ρ), and Sound Velocity[d] (c) of MEA (1) + H_2O (2) + bmim[OTF] (3) with Different Mass Compositions (w)

sample	A_1	A_2	A_3	AAD(η)	B_1	B_2	B_3	AAD(ρ)	D_1	D_2	AAD(c)
w_1 = 0.3004, w_2 = 0.6996	0.4156	132.5	227.5	0.003	-2.50×10^{-6}	0.001052	0.9188	0.0001	−0.5773	1846	1.9
w_1 = 0.3119, w_2 = 0.5837, w_3 = 0.1045	0.3102	193.5	219.6	0.008	-1.84×10^{-6}	0.0006	1.037	0.00003	−1.343	2097	1.3
w_1 = 0.2994, w_2 = 0.4614, w_3 = 0.2392	0.2081	286.6	208.2	0.009	-1.40×10^{-6}	0.0002	1.14	0.0001	−1.846	2237	0.6
w_1 = 0.3046, w_2 = 0.2642, w_3 = 0.4311	0.0446	746.6	158.8	0.007	-8.99×10^{-7}	−0.0002	1.268	0.0005	−2.287	2322	0.6

[a] $\mathrm{AAD}(x) = \frac{1}{N_p}\sum_1^{N_p} |x_{exp} - x_{cal}|$. [b] $\eta = A_1 \exp[\frac{A_2}{T - A_3}]$. [c] $\rho = B_1T^2 + B_2T + B_3$. [d] $c = D_1\ T + D_2$.

Table 13. Regressed Parameters and Statistical Deviations[a] (AAD) for Viscosity[b] (η), Density[c] (ρ), and Sound Velocity[d] (c) of MEA (1) + H_2O (2)/(NMP (2) + bmim[TF_2N] (3))/bmim[OTF] (3) with Different Mass Compositions (w)

sample	A_1	A_2	A_3	AAD(η)	B_1	B_2	B_3	AAD(ρ)	D_1	D_2	AAD(c)
w_1 = 0.0912, $w_{bmim[OTF]}$ = 0.9088	0.2244	635.8	176.7	0.076	3.00×10^{-7}	-9.929×10^{-4}	1.531	2.0×10^{-4}	−2.318	2120	0.3
w_1 = 0.1034, w_{water} = 0.8966	0.05118	409.9	169	0.001	-3.40×10^{-6}	1.724×10^{-3}	0.7898	1.0×10^{-4}	0.9452	1275	3.1
w_1 = 0.1021, w_{NMP} = 0.8979[e], w_1 = 0.1025, w_{NMP} = 0.8975[f]	0.4923	156.6	206.3	0.002	-1.42×10^{-7}	-8.083×10^{-4}	1.28	5.0×10^{-4}	−3.778	2685	0.4
w_1 = 0.2008, w_{water} = 0.7992	0.01185	956.6	105	0.005	-2.90×10^{-6}	1.387×10^{-3}	0.8533	1.0×10^{-4}	0.208	1554	2.8
w_1 = 0.2090, w_{NMP} = 0.7910[e], w_1 = 0.1990, w_{NMP} = 0.8010[f]	0.3834	208.5	199.5	0.004	-1.40×10^{-8}	-8.878×10^{-4}	1.292	4.0×10^{-4}	−3.745	2689	0.4
w_1 = 0.3089, w_{NMP} = 0.6911[e], w_1 = 0.3074, w_{NMP} = 0.6926[f]	0.2703	281.1	194.9	0.005	-8.30×10^{-8}	-8.354×10^{-4}	1.279	3.0×10^{-4}	−3.706	2691	0.3
w_1 = 0.0976, w_{NMP} = 0.8032, $w_{bmim[TF2N]}$ = 0.0992	0.4296	200.1	195.9	0.002	-3.00×10^{-7}	-7.155×10^{-4}	1.301	1.0×10^{-4}	−3.583	2604	0.6
w_1 = 0.1138, w_{NMP} = 0.6414, $w_{bmim[TF2N]}$ = 0.2448	0.2899	305.8	183.8	0.003	-5.00×10^{-7}	-6.251×10^{-4}	1.333	4.0×10^{-4}	−3.338	2490	0.4
w_1 = 0.1162, w_{NMP} = 0.4932, $w_{bmim[TF2N]}$ = 0.3906	0.1886	444.7	167.1	0.004	-3.00×10^{-7}	-7.642×10^{-4}	1.404	2.0×10^{-4}	−3.123	2378	0.3

[a] $\mathrm{AAD}(x) = \frac{1}{N_p}\sum_1^{N_p} |x_{exp} - x_{cal}|$. [b] $\eta = A_1 \exp[\frac{A_2}{T - A_3}]$. [c] $\rho = B_1T^2 + B_2T + B_3$. [d] $c = D_1\ T + D_2$. [e]Viscosity measurements. [f]Density and sound velocity measurements.

5. CONCLUSIONS

The performance of mixed solvents was investigated regarding the solubility of CO_2. Solubility data were measured for systems of CO_2 and MEA + H_2O + bmim[OTF] and MEA + NMP + bmim[TF_2N] at temperatures of 298.15 and 313.15 K in the pressure range of 0.093−2.322 MPa. Additionally, the viscosity, density, speed of sound, and evaporation rate of the liquid mixtures were also experimentally measured. Considering the aqueous MEA solvent, the replacement of the aqueous part of the solvent with NMP and IL increased the solubility of CO_2 at a pressure greater than 1.1 MPa. In all cases, the replacement with NMP alone provided the greatest increase in CO_2 solubility. Overall, the viscosity of the mixed solvents was greater than the aqueous MEA solvent, with the ILs greatly increasing the solvent viscosity. However, the inclusion of ILs to the chemical solvent seems to aid with the regeneration step at lower pressures. Further studies are needed on the other gas constituents and degradation temperatures.

AUTHOR INFORMATION

Corresponding Author

Wayne Michael Nelson − *Thermodynamics Research Unit, School of Engineering, University of KwaZulu-Natal, Durban 4040, South Africa;* orcid.org/0000-0003-0544-6530; Email: nelsonw@ukzn.ac.za

Authors

Mojgan Ebrahiminejadhasanabadi − *Thermodynamics Research Unit, School of Engineering, University of KwaZulu-Natal, Durban 4040, South Africa*

Paramespri Naidoo − *Thermodynamics Research Unit, School of Engineering, University of KwaZulu-Natal, Durban 4040, South Africa;* orcid.org/0000-0002-2724-7308

Amir H. Mohammadi − *Thermodynamics Research Unit, School of Engineering, University of KwaZulu-Natal, Durban 4040, South Africa;* orcid.org/0000-0002-2947-1135

Deresh Ramjugernath − *Thermodynamics Research Unit, School of Engineering, University of KwaZulu-Natal, Durban 4040, South Africa;* orcid.org/0000-0003-3447-7846

Complete contact information is available at: https://pubs.acs.org/10.1021/acs.jced.0c00618

Notes

The authors declare no competing financial interest.

ACKNOWLEDGMENTS

This work is based upon research supported by the National Research Foundation of South Africa under the South African Research Chair Initiative of the Department of Science and Technology, Grant UID number: 64817.

REFERENCES

(1) Karadas, F.; Atilhan, M.; Aparicio, S. Review on the Use of Ionic Liquids (ILs) as Alternative Fluids for CO_2 Capture and Natural Gas Sweetening. *Energy Fuels* **2010**, *24*, 5817−5828.

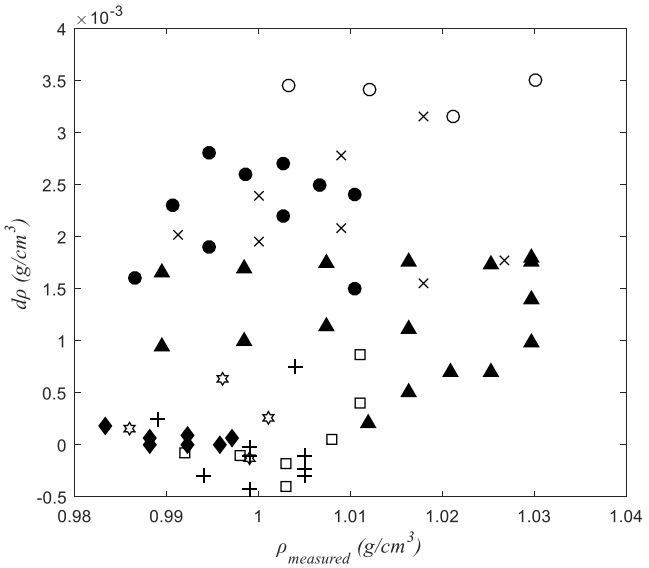

Figure 6. Density deviation ($d\rho = \rho_{measured} - \rho_{literature}$) versus measured density for MEA (1) + H_2O (2) with mass fractions: $w_1 \approx 0.10$ at 298.15, 303.15, 313.15, and 333.15 K (☆),[68] $w_1 \approx 0.20$ at 298.15, 303.15, 313.15, 323.15, and 333.15 K (+);[64,68,69] $w_1 \approx 0.30$ at 298.15, 303.15, 313.15, 323.15, and 333.15 K (□);[64,68] MEA (1) + NMP (2) with mass fractions: $w_1 \approx 0.2$ at 293.15, 303.15, 313.15, and 323.15 K (○)[66] and $w_1 \approx 0.30$ at 293.15, 303.15, 313.15, 323.15, and 333.15 K (×);[66,67] MEA at 303.15, 308.15, 313.15, 318.15, 323.15, 328.15, and 333.15 K (●);[67,70] NMP at 298.15, 303.15, 308.15, 313.15, 318.15, 323.15, 333.15, and 343.15 K (▲);[45,71−73] and water at 298.15, 303.15, 313.15, 323.15, and 333.15 K (♦).[70,74]

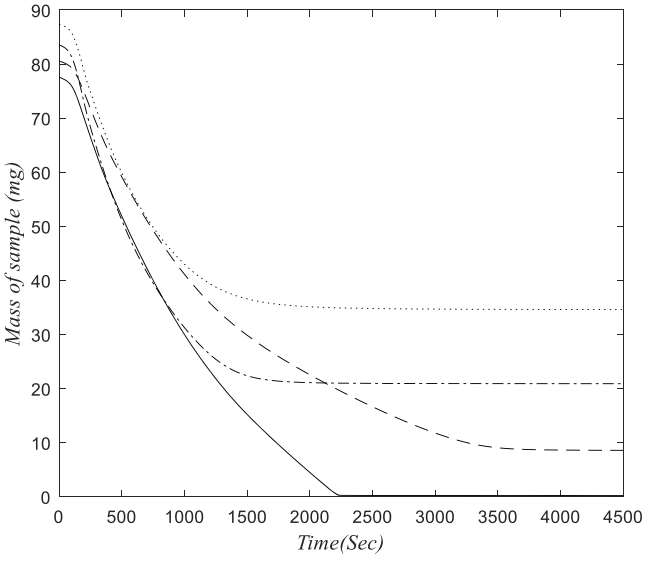

Figure 7. Sample mass versus time at a temperature of 373.15 K for mixtures of MEA (1) + H_2O (2) + bmim[OTF] (3) with different mass compositions: $w_2/w_1 = 0.6996/0.3004$ (solid line), $w_3/w_2/w_1 = 0.1045/0.58336/0.3119$ (dashed line), $w_3/w_2/w_1 = 0.2492/0.458/0.2928$ (dash-dot line) and $w_3/w_2/w_1 = 0.3943/0.3178/0.2879$ (dotted line).

(2) Demirbas, A. *Methane Gas Hydrate*; Springer, 2010.
(3) International Energy Agency. *World Energy Outlook (WEO) 2017 (New Policies Scenario)*; 2017.
(4) Faramawy, S.; Zaki, T.; Sakr, A. A. E. Natural Gas Origin, Composition, and Processing: A Review. *J. Nat. Gas Sci. Eng.* **2016**, *34*, 34−54.
(5) Haghtalab, A.; Izadi, A. Solubility and Thermodynamic Modeling of Hydrogen Sulfide in Aqueous (Diisopropanolamine + 2-Amino-2-methyl-1-propanol + Piperazine) Solution at High Pressure. *J. Chem. Thermodyn.* **2015**, *90*, 106−115.
(6) Haghtalab, A.; Izadi, A. Simultaneous Measurement Solubility of Carbon Dioxide + Hydrogen Sulfide into Aqueous Blends of Alkanolamines at High Pressure. *Fluid Phase Equilib.* **2014**, *375*, 181−190.
(7) Bhide, B. D.; Voskericyan, A.; Stern, S. A. Hybrid Processes for the Removal of Acid Gases from Natural Gas. *J. Membr. Sci.* **1998**, *140*, 27−49.
(8) Shimekit, B.; Mukhtar, H. Natural Gas Purification Technologies - Major Advances for CO_2 Separation and Future Directions. In *Advances in Natural Gas Technology*; Al-Megren, H., Ed.; InTech, 2012; pp 235−270.
(9) Torralba-Calleja, E.; Skinner, J.; Gutiérrez-Tauste, D. CO_2 Capture in Ionic Liquids: A Review of Solubilities and Experimental Methods. *J. Chem.* **2013**, *2013*, 1−16.
(10) Guo, B.; Duan, E.; Zhong, Y.; Gao, L.; Zhang, X.; Zhao, D. Absorption and Oxidation of H_2S in Caprolactam Tetrabutyl Ammonium Bromide Ionic Liquid. *Energy Fuels* **2011**, *25*, 159−161.
(11) Jalili, A. H.; Rahmati-Rostami, M.; Ghotbi, C.; Hosseini-Jenab, M.; Ahmadi, A. N. Solubility of H_2S in Ionic Liquids [bmim][PF_6], [bmim][BF_4], and [bmim][Tf_2N]. *J. Chem. Eng. Data* **2009**, *54*, 1844−1849.
(12) Baj, S.; Siewniak, A.; Chrobok, A.; Krawczyk, T.; Sobolewski, A. Monoethanolamine and Ionic Liquid Aqueous Solutions as Effective Systems for CO_2 Capture. *J. Chem. Technol. Biotechnol.* **2013**, *88*, 1220−1227.
(13) Lu, B.-H.; Jin, J.-J.; Zhang, L.; Li, W. Absorption of Carbon Dioxide into Aqueous Blend of Monoethanolamine and 1-Butyl-3-methylimidazolium Tetrafluoroborate. *Int. J. Greenhouse Gas Control* **2012**, *11*, 152−157.
(14) Shojaeian, A.; Haghtalab, A. Solubility and Density of Carbon Dioxide in Different Aqueous Alkanolamine Solutions Blended with 1-Butyl-3-methylimidazolium Acetate Ionic Liquid at High Pressure. *J. Mol. Liq.* **2013**, *187*, 218−225.
(15) Kumar, S.; Cho, J. H.; Moon, I. Ionic Liquid-amine Blends and CO_2BOLs: Prospective Solvents for Natural Gas Sweetening and CO_2 Capture Technology—A Review. *Int. J. Greenhouse Gas Control* **2014**, *20*, 87−116.
(16) Akbar, M. M.; Murugesan, T. Thermophysical Properties for the Binary Mixtures of 1-Hexyl-3-methylimidazolium Bis-(trifluoromethylsulfonyl)imide [hmim][Tf_2N] + N-methyldiethanolamine (MDEA) at Temperatures (303.15 to 323.15) K. *J. Mol. Liq.* **2012**, *169*, 95−101.
(17) Huang, K.; Wu, Y.-T.; Hu, X.-B. Effect of Alkalinity on Absorption Capacity and Selectivity of SO_2 and H_2S over CO_2: Substituted Benzoate-based Ionic Liquids as the Study Platform. *Chem. Eng. J.* **2016**, *297*, 265−276.
(18) Yokozeki, A.; Shiflett, M. B.; Junk, C. P.; Grieco, L. M.; Foo, T. Physical and Chemical Absorptions of Carbon Dioxide in Room-Temperature Ionic Liquids. *J. Phys. Chem. B* **2008**, *112*, 16654−16663.
(19) Pomelli, C. S.; Chiappe, C.; Vidis, A.; Laurenczy, G.; Dyson, P. J. Influence of the Interaction between Hydrogen Sulfide and Ionic Liquids on Solubility: Experimental and Theoretical Investigation. *J. Phys. Chem. B* **2007**, *111*, 13014−13019.
(20) Haghtalab, A.; Shojaeian, A. High Pressure Measurement and Thermodynamic Modelling of the Solubility of Carbon Dioxide in N-methyldiethanolamine and 1-Butyl-3-methylimidazolium Acetate Mixture. *J. Chem. Thermodyn.* **2015**, *81*, 237−244.
(21) Bernard, F. L.; Dalla Vecchia, F.; Rojas, M. F.; Ligabue, R.; Vieira, M. O.; Costa, E. M.; Chaban, V. V.; Einloft, S. Anticorrosion Protection by Amine−Ionic Liquid Mixtures: Experiments and Simulations. *J. Chem. Eng. Data* **2016**, *61*, 1803−1810.
(22) Ahmady, A.; Hashim, M. A.; Aroua, M. K. Kinetics of Carbon Dioxide Absorption into Aqueous MDEA + [bmim][BF_4] solutions from 303 to 333K. *Chem. Eng. J.* **2012**, *200-202*, 317−328.

https://dx.doi.org/10.1021/acs.jced.0c00618
J. Chem. Eng. Data 2021, 66, 899−914

Table 14. Experimental Data Describing the Samples of MEA (1) + H_2O (2) + bmim[OTF] (3) Mixtures with Different Initial Mass Compositions and $U(w)$ = 0.0001 Used for TGA Measurements[a]

sample	initial mass (mg)	initial MEA (mg)	initial water (mg)	initial IL (mg)	final mass after 75 min (mg)	estimated evaporation rate of water (mg/s)	estimated evaporation rate of MEA (mg/s)
w_1 = 0.3004, w_2 = 0.6996	77.5779	23.3048	54.2731	0	0.2042	0.0452	0.0221
w_1 = 0.3119, w_2 = 0.5837, w_3 = 0.1045	80.5632	25.1242	47.0215	8.4175	8.5727	0.0360	0.0106
w_1 = 0.2928, w_2 = 0.4581, w_3 = 0.2492	83.5133	24.4488	38.2565	20.8080	20.8975	0.0623	0.0191
w_1 = 0.2879, w_2 = 0.3177, w_3 = 0.3943	87.3554	25.1520	27.7565	34.4469	34.5976	0.0548	0.0150

[a]Readability = 0.0001 mg, sensitivity = 0.001 mg.

Table 15. Experimental Data Describing the Samples of MEA (1) + H_2O (2)/(NMP (2) + bmim[TF_2N] (3))/bmim[OTF] (2) Mixtures with Different Initial Mass Compositions and $U(w)$ = 0.0001 Used for TGA Measurements[a]

sample	initial mass (mg)	initial MEA (mg)	initial NMP/water (mg)	initial IL (mg)	final mass (mg)	final point for time (h)	total evaporation rate of MEA and NMP (mg/s)
w_1 = 0.0912, $w_{bmim[OTF]}$ = 0.9088	98.2988	8.9604	0.0000	89.3384	88.5057	6.44	0.0023
w_1 = 0.0997, w_{water} = 0.9003	80.9731	8.0746	72.8985	0.0000	0.2184	0.53	0.0235[b]
w_1 = 0.1129, w_{NMP} = 0.8871	85.0610	9.6008	75.4602	0.0000	0.9337	6.36	0.0139
w_1 = 0.2070, w_{NMP} = 0.7930	84.2621	17.4412	66.8209	0.0000	1.3081	1.95	0.0144
w_1 = 0.1985, w_{water} = 0.8015	76.7235	15.2276	61.4960	0.0000	0.1512	0.67	0.0247[b]
w_1 = 0.3050, w_{NMP} = 0.6950	83.7564	25.5446	58.2118	0.0000	1.7780	1.93	0.0151
w_1 = 0.3004, w_{water} = 0.6996	77.5779	23.3048	54.2731	0.0000	0.2042	1.25	0.0221[b]
w_1 = 0.1039, w_{NMP} = 0.7966, $w_{bmim[TF2N]}$ = 0.0995	85.4334	8.8763	68.0590	8.4980	8.4551	8.36	0.0190
w_1 = 0.0977, w_{NMP} = 0.6492, $w_{bmim[TF2N]}$ = 0.2531	84.1945	8.2257	54.6603	21.3085	21.2525	8.36	0.0113
w_1 = 0.1162, w_{NMP} = 0.4932, $w_{bmim[TF2N]}$ = 0.3906	89.1767	10.3618	43.9823	34.8326	34.4382	9.55	0.0086

[a]Readability = 0.0001 mg, sensitivity = 0.001 mg. [b]Estimated evaporation rate of MEA (mg/s).

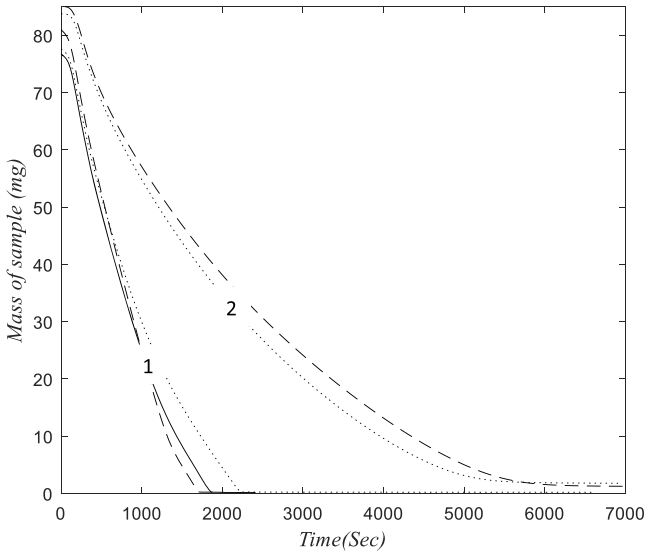

Figure 8. Sample mass versus time at a temperature of 373.15 K for MEA (1) + H_2O (2) mixtures with different mass compositions (group 1): w_1/w_2 = 0.0997/0.9003 (dashed line), w_1/w_2 = 0.1985/0.8015 (solid line), w_1/w_2 = 0.3004/0.6996 (dotted line), and mixtures of MEA (1) + NMP (2) with mass fractions (group 2): w_1/w_2 = 0.1129/0.8871 (dashed line), w_1/w_2 = 0.2070/0.793 (solid line), w_1/w_2 = 0.3050/0.695 (dotted line).

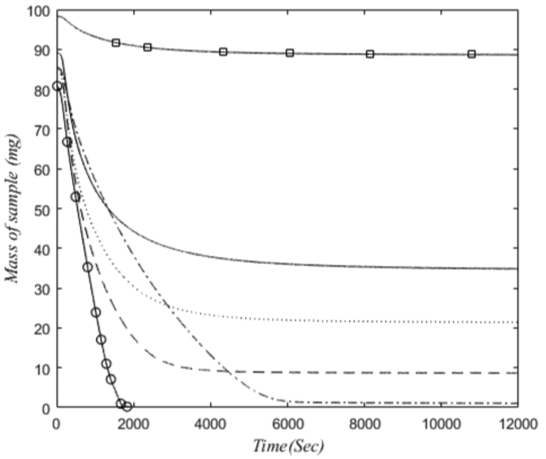

Figure 9. Sample mass versus time at a temperature of 373.15 K for MEA (1) + NMP (2) + bmim[TF_2N] (3) mixtures with different mass compositions: w_1/w_2 = 0.1129/0.8871 (dash-dot line), $w_1/w_2/w_3$ = 0.1039/0.7966/0.0995 (dashed line), $w_1/w_2/w_3$ = 0.0977/0.6492/0.2531 (dotted line) and $w_1/w_2/w_3$ = 0.1162/0.4932/0.3906 (solid line); MEA (1) + bmim[OTF] (2) with mass fraction w_1/w_2 = 0.0912/0.9088 (□); and mixture of MEA (2) + H_2O (3) with mass fraction: w_1/w_2 = 0.0997/0.900 (○).

(23) Gao, J.; Cao, L.; Dong, H.; Zhang, X.; Zhang, S. Ionic Liquids Tailored Amine Aqueous Solution for Pre-combustion CO_2 Capture: Role of Imidazolium-based Ionic Liquids. *Appl. Energy* **2015**, *154*, 771−780.

(24) Yang, J.; Yu, X.; Yan, J.; Tu, S.-T. CO_2 Capture Using Amine Solution Mixed with Ionic Liquid. *Ind. Eng. Chem. Res.* **2014**, *53*, 2790−2799.

(25) McCrellis, C.; Taylor, S. F. R.; Jacquemin, J.; Hardacre, C. Effect of the Presence of MEA on the CO_2 Capture Ability of Superbase Ionic Liquids. *J. Chem. Eng. Data* **2016**, *61*, 1092−1100.

https://dx.doi.org/10.1021/acs.jced.0c00618
J. Chem. Eng. Data 2021, 66, 899−914

(26) Ahmady, A.; Hashim, M. A.; Aroua, M. K. Absorption of Carbon Dioxide in the Aqueous Mixtures of Methyldiethanolamine with Three Types of Imidazolium-based Ionic Liquids. *Fluid Phase Equilib.* **2011**, *309*, 76−82.
(27) Aziz, N.; Yusoff, R.; Aroua, M. K. Absorption of CO_2 in Aqueous Mixtures of N-methyldiethanolamine and Guanidinium Tris(pentafluoroethyl)trifluorophosphate Ionic Liquid at High-Pressure. *Fluid Phase Equilib.* **2012**, *322-323*, 120−125.
(28) Iliuta, I.; Hasib-ur-Rahman, M.; Larachi, F. CO_2 Absorption in Diethanolamine/Ionic Liquid Emulsions − Chemical Kinetics and Mass Transfer Study. *Chem. Eng. J.* **2014**, *240*, 16−23.
(29) Li, Y.; Zheng, D.; Dong, L.; Nie, N.; Xiong, B. Solubilities of CO_2 in, and Densities and Viscosities of, the Piperazine + 1-Ethyl-3-methyl-imidazolium Acetate + H_2O System. *J. Chem. Eng. Data* **2014**, *59*, 618−625.
(30) Xiao, M.; Liu, H.; Gao, H.; Olson, W.; Liang, Z. CO_2 Capture with Hybrid Absorbents of Low Viscosity Imidazolium-based Ionic Liquids and Amine. *Appl. Energy* **2019**, *235*, 311−319.
(31) Xu, F.; Gao, H.; Dong, H.; Wang, Z.; Zhang, X.; Ren, B.; Zhang, S. Solubility of CO_2 in Aqueous Mixtures of Monoethanolamine and Dicyanamide-based Ionic Liquids. *Fluid Phase Equilib.* **2014**, *365*, 80−87.
(32) Lu, B.; Wang, X.; Xia, Y.; Liu, N.; Li, S.; Li, W. Kinetics of Carbon Dioxide Absorption into Mixed Aqueous Solutions of MEA + [Bmim]BF_4 Using a Double Stirred Cell. *Energy Fuels* **2013**, *27*, 6002−6009.
(33) Ahmady, A.; Hashim, M. A.; Aroua, M. K. Experimental Investigation on the Solubility and Initial Rate of Absorption of CO_2 in Aqueous Mixtures of Methyldiethanolamine with the Ionic Liquid 1-Butyl-3-methylimidazolium Tetrafluoroborate. *J. Chem. Eng. Data* **2010**, *55*, 5733−5738.
(34) Sairi, N. A.; Yusoff, R.; Alias, Y.; Aroua, M. K. Solubilities of CO_2 in Aqueous N-methyldiethanolamine and Guanidinium Trifluoromethanesulfonate Ionic Liquid Systems at Elevated Pressures. *Fluid Phase Equilib.* **2011**, *300*, 89−94.
(35) Feng, Z.; Cheng-Gang, F.; You-Ting, W.; Yuan-Tao, W.; Ai-Min, L.; Zhi-Bing, Z. Absorption of CO_2 in the Aqueous Solutions of Functionalized Ionic Liquids and MDEA. *Chem. Eng. J.* **2010**, *160*, 691−697.
(36) Feng, Z.; Jing-Wen, M.; Zheng, Z.; You-Ting, W.; Zhi-Bing, Z. Study on the Absorption of Carbon Dioxide in High Concentrated MDEA and ILs Solutions. *Chem. Eng. J.* **2012**, *181-182*, 222−228.
(37) Hasib-ur-Rahman, M.; Larachi, F. Kinetic Behavior of Carbon Dioxide Absorption in Diethanolamine/Ionic-Liquid Emulsions. *Sep. Purif. Technol.* **2013**, *118*, 757−761.
(38) Feng, Z.; Yuan, G.; Xian-Kun, W.; Jing-Wen, M.; You-Ting, W.; Zhi-Bing, Z. Regeneration Performance of Amino Acid Ionic Liquid (AAIL) Activated MDEA Solutions for CO_2 Capture. *Chem. Eng. J.* **2013**, *223*, 371−378.
(39) Gao, Y.; Zhang, F.; Huang, K.; Ma, J.-W.; Wu, Y.-T.; Zhang, Z.-B. Absorption of CO_2 in Amino Acid Ionic Liquid (AAIL) Activated MDEA Solutions. *Int. J. Greenhouse Gas Control* **2013**, *19*, 379−386.
(40) Ghani, N. A.; Sairi, N. A.; Aroua, M. K.; Alias, Y.; Yusoff, R. Density, Surface Tension, and Viscosity of Ionic Liquids (1-Ethyl-3-methylimidazolium Diethylphosphate and 1,3-Dimethylimidazolium Dimethylphosphate) Aqueous Ternary Mixtures with MDEA. *J. Chem. Eng. Data* **2014**, *59*, 1737−1746.
(41) Aparicio, S.; Atilhan, M. Water Effect on CO_2 Absorption for Hydroxylammonium Based Ionic Liquids: A Molecular Dynamics Study. *Chem. Phys.* **2012**, *400*, 118−125.
(42) Yang, J.; Yu, X.; An, L.; Tu, S.-T.; Yan, J. CO_2 Capture with the Absorbent of a Mixed Ionic Liquid and Amine Solution Considering the Effects of SO_2 and O_2. *Appl. Energy* **2017**, *194*, 9−18.
(43) Lei, Z.; Zhang, B.; Zhu, J.; Gong, W.; LÜ, J.; Li, Y. Solubility of CO_2 in Methanol, 1-Octyl-3-methylimidazolium Bis-(trifluoromethylsulfonyl)imide, and Their Mixtures. *Chin. J. Chem. Eng.* **2013**, *21*, 310−317.
(44) Shokouhi, M.; Hosseini-Jenab, M.; Mehdizadeh, A.; Naser Ahmadi, A.; Jalili, A. H. Experimental Investigation on the Solubility and Initial Rate of Absorption of CO_2 in Mixture of Amine-Functionalized Ionic Liquids and Physical Solvents. *Iran. J. Chem. Eng.* **2015**, *12*, 68−77.
(45) Tian, S.; Hou, Y.; Wu, W.; Ren, S.; Pang, K. Physical Properties of 1-Butyl-3-methylimidazolium Tetrafluoroborate/N-Methyl-2-pyrrolidone Mixtures and the Solubility of CO_2 in the System at Elevated Pressures. *J. Chem. Eng. Data* **2012**, *57*, 756−763.
(46) Mushtaq, A.; Mukhtar, H. B.; Shariff, A. M.; Mannan, H. A. A Review: Fabrication of Enhanced Polymeric Blend Membrane with Amines for Removal of CO_2 from Natural Gas. *IJETAE* **2013**, *3*, 529−551.
(47) Kohl, A.; Nielsen, R. *Gas Purification*; Gulf Publishing Company: Houston, Texas, 1997.
(48) Burr, B.; Lyddon, L. *A Comparison of Physical Solvents for Acid Gas Removal;* Bryan Research & Engineering, Inc., 2008.
(49) Ebrahiminejadhasanabadi, M. Solubility studies of carbon dioxide in novel hybrid solvents using a new static synthetic apparatus. Doctoral dissertation, University of KwaZulu-Natal: Durban, South Africa, 2020.
(50) Kidnay, A. J.; Parrish, W. R. *Fundamentals of Natural Gas Processing*; Taylor & Francis Group: United States of America, Columbus, 2011.
(51) Pars Oil and Gas Company. *Oil and gas processing plant design and operation training course: gas sweetening processes*; Excerpt from PRODEM, 2002.
(52) Mohd Salleh, R. Volumetric Properties and Absorption of Carbon Dioxide in Aqueous Solutions of Piperazine and Activated Diethanolamine. Doctoral dissertation, University of Malaya: Kuala Lumpur, Malaysia, 2005.
(53) Gate. H_2S Scavenging: Amine Systems. https://gate.energy/the-arrow-blog/pme/cse/gat2004-gkp-2014-06/h2s-scavenging-amine-systems, 2014.
(54) Polasek, J.; Bullin, J. A. *Selecting Amines for Sweetening Units*; Bryan Research and Engineering, Inc., 2006.
(55) Newpoint Gas. Amine Treating Plants. https://www.newpointgas.com/services/amine-treating-plants/, 2017.
(56) Ebrahiminejadhasanabadi, M.; Nelson, W. M.; Naidoo, P.; Mohammadi, A. H.; Ramjugernath, D. Experimental Measurement of Carbon Dioxide Solubility in 1-Methylpyrrolidin-2-one (NMP) + 1-Butyl-3-methyl-1H-imidazol-3-ium Tetrafluoroborate ([bmim][BF_4]) Mixtures Using a New Static-Synthetic Cell. *Fluid Phase Equilib.* **2018**, *477*, 62−77.
(57) Lazzaroni, M. J.; Bush, D.; Brown, J. S.; Eckert, C. A. High-Pressure Vapor−Liquid Equilbria of Some Carbon Dioxide + Organic Binary Systems. *J. Chem. Eng. Data* **2005**, *50*, 60−65.
(58) Taylor, B. N.; Kuyatt, C. E. *NIST Technical Note 1297: Guidelines for Evaluating and Expressing the Uncertainty of NIST Measurement Results*; National Institute of Standards and Technology: Gaithersburg, 1994.
(59) Harris, K. R.; Kanakubo, M.; Woolf, L. A. Temperature and Pressure Dependence of the Viscosity of the Ionic Liquids 1-Hexyl-3-methylimidazolium Hexafluorophosphate and 1-Butyl-3-methylimidazolium Bis(trifluoromethylsulfonyl)imide. *J. Chem. Eng. Data* **2007**, *52*, 1080−1085.
(60) Mokhtarani, B.; Sharifi, A.; Mortaheb, H. R.; Mirzaei, M.; Mafi, M.; Sadeghian, F. Density and Viscosity of Pyridinium-based Ionic Liquids and Their Binary Mixtures with Water at Several Temperatures. *J. Chem. Thermodyn.* **2009**, *41*, 323−329.
(61) Zhao, Y.; Zhang, X.; Zeng, S.; Zhou, Q.; Dong, H.; Tian, X.; Zhang, S. Density, Viscosity, and Performances of Carbon Dioxide Capture in 16 Absorbents of Amine + Ionic Liquid + H_2O, Ionic Liquid + H_2O, and Amine + H_2O Systems. *J. Chem. Eng. Data* **2010**, *55*, 3513−3519.
(62) Rivas, O. R.; Prausnitz, J. M. Sweetening of sour natural gases by mixed-solvent absorption: Solubilities of ethane, carbon dioxide, and hydrogen sulfide in mixtures of physical and chemical solvents. *AICHE J.* **1979**, *25*, 975−984.

https://dx.doi.org/10.1021/acs.jced.0c00618
J. Chem. Eng. Data 2021, 66, 899−914

(63) Peyghambarzadeh, S. M.; Jamialahmadi, M.; Alavi Fazel, S. A.; Azizi, S. Experimental and theoretical study of pool boiling heat transfer to amine solutions. *Braz. J. Chem. Eng.* **2009**, *26*, 33−43.
(64) Amundsen, T. G.; Øi, L. E.; Eimer, D. A. Density and Viscosity of Monoethanolamine + Water + Carbon Dioxide from (25 to 80) °C. *J. Chem. Eng. Data* **2009**, *54*, 3096−3100.
(65) Arachchige, U. S. P. R.; Aryal, N.; Eimer, D. A.; Melaaen, M. C. Viscosities of Pure and Aqueous Solutions of Monoethanolamine (MEA), Diethanolamine (DEA) and N-Methyldiethanolamine (MDEA). *Annu. Trans. - Nord. Rheol. Soc.* **2013**, *21*, 299−306.
(66) García-Abuín, A.; Gómez-Díaz, D.; La Rubia, M. D.; Navaza, J. M. Density, Speed of Sound, Viscosity, Refractive Index, and Excess Volume of N-methyl-2-pyrrolidone + Ethanol (or Water or Ethanolamine) from T = (293.15 to 323.15) K. *J. Chem. Eng. Data* **2011**, *56*, 646−651.
(67) Águila-Hernández, J.; Trejo, A.; García-Flores, B. E.; Molnar, R. Viscometric and volumetric behaviour of binary mixtures of sulfolane and N-methylpyrrolidone with monoethanolamine and diethanolamine in the range 303−373 K. *Fluid Phase Equilib.* **2008**, *267*, 172−180.
(68) Maham, Y.; Teng, T. T.; Hepler, L. G.; Mather, A. E. Densities, excess molar volumes, and partial molar volumes for binary mixtures of water with monoethanolamine, diethanolamine, and triethanolamine from 25 to 80°C. *J. Solution Chem.* **1994**, *23*, 195−205.
(69) Pagé, M.; Huot, J. Y.; Jolicoeur, C. A comprehensive thermodynamic investigation of water−ethanolamine mixtures at 10, 25, and 40 °C. *Can. J. Chem.* **1993**, *71*, 1064−1072.
(70) Lee, M.-J.; Lin, T.-K. Density and Viscosity for Monoethanolamine + Water, + Ethanol, and + 2-Propanol. *J. Chem. Eng. Data* **1995**, *40*, 336−339.
(71) Henni, A.; Hromek, J. J.; Tontiwachwuthikul, P.; Chakma, A. Volumetric Properties and Viscosities for Aqueous N-Methyl-2-pyrrolidone Solutions from 25 °C to 70 °C. *J. Chem. Eng. Data* **2004**, *49*, 231−234.
(72) Pal, A.; Bhardwaj, R. K. Excess Molar Volumes and Viscosities for Binary Mixtures of 2-Propoxyethanol and of 2-Isopropoxyethanol with Propylamine and Dipropylamine at (298.15, 308.15, and 318.15) K. *J. Chem. Eng. Data* **2001**, *46*, 933−938.
(73) Yang, C.; Liu, Z.; Lai, H.; Ma, P. Thermodynamic properties of binary mixtures of N-methyl-2-pyrrolidinone with cyclohexane, benzene, toluene at (303.15 to 353.15)K and atmospheric pressure. *J. Chem. Thermodyn.* **2007**, *39*, 28−38.
(74) Henni, A.; Tontiwachwuthikul, P.; Chakma, A.; Mather, A. E. Volumetric Properties and Viscosities for Aqueous Diglycolamine Solutions from 25 °C to 70 °C. *J. Chem. Eng. Data* **2001**, *46*, 56−62.
(75) Zhou, Q.; Wang, L.-S.; Chen, H.-P. Densities and Viscosities of 1-Butyl-3-methylimidazolium Tetrafluoroborate + H_2O Binary Mixtures from (303.15 to 353.15) K. *J. Chem. Eng. Data* **2006**, *51*, 905−908.
(76) Khan, S. N.; Hailegiorgis, S. M.; Man, Z.; Shariff, A. M.; Garg, S. Thermophysical Properties of Aqueous N-methyldiethanolamine (MDEA) and Ionic Liquids 1-Butyl-3-methylimidazolium Trifluoromethanesulfonate [bmim][OTf], 1-Butyl-3-methylimidazolium Acetate [bmim][Ac] Hybrid Solvents for CO_2 Capture. *Chem. Eng. Res. Des.* **2017**, *121*, 69−80.
(77) García, S.; Larriba, M.; García, J.; Torrecilla, J. S.; Rodríguez, F. Liquid−Liquid Extraction of Toluene from Heptane Using 1-Alkyl-3-methylimidazolium Bis(trifluoromethylsulfonyl)imide Ionic Liquids. *J. Chem. Eng. Data* **2011**, *56*, 113−118.
(78) Tseng, Y.-M.; Thompson, A. R. Densities and Refractive Indices of Aqueous Monoethanolamine, Diethanolamine, Triethanolamine. *J. Chem. Eng. Data* **1964**, *9*, 264−267.

https://dx.doi.org/10.1021/acs.jced.0c00618
J. Chem. Eng. Data 2021, 66, 899−914